Extended-soft-core baryon-baryon model. I. Nucleon-nucleon scattering with the ESC04 interaction

Th. A. Rijken*

Institute for Mathematics, Astrophysics, and Particle Physics, Radboud University, Nijmegen, The Netherlands

(Received 14 October 2005; published 14 April 2006)

The *NN* results are presented from the extended-soft-core (ESC) interactions. They consist of local and nonlocal potentials due to (i) one-boson-exchanges (OBE), which are the members of nonets of pseudoscalar, vector, scalar, and axial mesons, (ii) diffractive exchanges, (iii) two-pseudoscalar exchanges (PS-PS), and (iv) meson-pair exchanges (MPE). We describe a fit to the *pp* and *np* data for $0 \leqslant T_{\rm lab} \leqslant 350$ MeV, having a typical $\chi^2/N_{\rm data} = 1.155$. Here, we used ∼20 quasi-free physical parameters, which are coupling constants and cutoff masses. A remarkable feature of the couplings is that we were able to require them to follow rather closely the pattern predicted by the $^3P_0$ quark-pair-creation (QPC) model. As a result the 11 OBE couplings are rather constrained, i.e., quasi free. Also, the deuteron binding energy and the several *NN* scattering lengths are fitted.

DOI: 10.1103/PhysRevC.73.044007 PACS number(s): 21.30.−x, 13.75.Cs, 12.39.Pn

I. INTRODUCTION

In a series of three papers we present the results recently obtained with the extended-soft-core (ESC) model [1] for nucleon-nucleon (*NN*), hyperon-nucleon (*YN*), and hyperon-hyperon (*YY*) data with $S = -2$. For *NN* [1–5] it has been demonstrated that the ESC-model interactions give an excellent description of the *NN*-data. Also, for *YN* the first attempts [6,7] showed that the ESC approach is potentially rather promising to give improvements with respect to the one-boson-exchange (OBE) soft-core models [8,9]. As compared with the earlier versions of the ESC model, we introduce in these papers two innovations. First, we introduce a zero in the form factor of the scalar mesons. Second, we exploit the exchange of the axial-vector mesons. In this first paper of the series, we display recent results fitting exclusively the *NN* data, giving the *NN* model presented in this paper, ESC04(*NN*). In the second paper, henceforth referred to as II [10], we report the results for $NN \oplus YN$, in a simultaneous fit of the *NN* and *YN* data. This is new with regard to our procedure described in previous publications on the Nijmegen work. The advantages will be discussed in II. In the third paper, henceforth referred to as III [11], we report the predictions for *YN* and *YY* with $S = -2$.

A general modern theoretical framework for the soft-core interactions is provided by the so-called standard model (SM). Starting from the SM, we consider the stage where the heavy quarks are integrated out, leaving an effective QCD world for the u, d, s quarks. The generally accepted scenario is now that the QCD vacuum is unstable for momentum transfers for which $Q^2 \leqslant \Lambda^2_{\chi\rm SB} \approx 1$ GeV^2 [12], causing spontaneous chiral-symmetry breaking (χSB). A phase transition of the vacuum generates constituent quark masses via $\langle 0|\bar\psi\psi|0\rangle \neq 0$, and thereby the gluon coupling α_s is reduced substantially. In view of the small pion mass, the Nambu-Goldstone bosons associated with the spontaneous χSB are naturally identified with the pseudoscalar mesons. Also, as a result of the phase transition the dominating degrees of freedom are the baryons and mesons. In this context, low-energy baryon-baryon interactions are described naturally by meson exchange by using form factors at the meson-baryon vertices. This way, the phase transition has transformed the effective QCD world into an effective hadronic world. To reduce this complex world with its numerous degrees of freedom, we consider a next step: envisioning integrating out of the heavy mesons and baryons by using a renormalization procedure a la Wilson [13], we restrict ourselves to mesons with $M \leqslant 1$ GeV$/c^2$, arriving at a so-called *effective field theory* as the proper arena to describe low-energy baryon-baryon scattering. This is the general physical basis for the Nijmegen soft-core models.

Because of the composite nature of the mesons in QCD, the proper description of meson exchange is quite naturally in terms of Regge trajectories. For example, in the Bethe-Salpeter approach to the $Q\bar Q$ system any reasonable interaction leads to Regge poles. Therefore, in the Nijmegen soft-core approach meson exchange is treated as the dominant part of the mesonic reggeon exchange. This includes also the $J = 0$ contributions from the tensor trajectories (f_2, f_2', and A_2). In elastic scattering we notice that the most important exchange at higher energies is pomeron exchange. Therefore in the soft-core OBE models [14] the traditional OBE model was extended by including the pomeron, and the pomeron parameters determined from the low-energy *NN* data were in good agreement with those found at high energy. This feature is also found to persist in the ESC models. For a more elaborate discussion of the pomeron and its importance for the implementation of chiral symmetry in the soft-core models, we refer to Refs. [8,15].

The dynamics in the ESC model is constructed by employing the following mesons together with *flavor* SU(3) symmetry:

(i) The pseudoscalar-meson nonet π, η, η', K with the $\eta - \eta'$ mixing angle $\theta_P = -23.0^\circ$ from the Gell-Mann-Okubo mass formula.
(ii) The vector-meson nonet $\rho, \phi, K^\star, \omega$ with the $\phi - \omega$ ideal mixing angle $\theta_V = 37.56^\circ$.
(iii) The axial-vector-meson nonet a_1, $f_1 K_1$, f_1' with the $f_1 - f_1'$ mixing angle $\theta_A = 47.3^\circ$ [4].

*Electronic address: t.rijken@science.ru.nl

(iv) The scalar-meson nonet $a_0(962) = \delta$, $f_0(993) = S^\star$, κ, $f_0(760) = \varepsilon$ with a free $S^\star - \varepsilon$ mixing angle θ_S to be determined in a fit to the *YN* data.

(v) The diffractive contribution from the pomeron P, and the tensor mesons f_2, f_2', and A_2. These interactions will give mainly repulsive contributions of a Gaussian type to the potentials in all channels. In the present ESC model we have taken $g_{A_2} = g_{BBf_2} = g_{BBf_2'} = 0$; i.e., only the pomeron contributes.

The BBM vertices are described by (i) coupling constants and $F/(F + D)$ ratios obeying broken flavor SU(3)-symmetry (see paper II for details) and (ii) Gaussian form factors. This type of form factor is like the often used residue functions in Regge phenomenology. Also, from the point of view of the (nonrelativistic) quark models a Gaussian behavior of the form factors is most natural. Here, we remark that in the ESC models the two-meson-cut contributions to the form factors are taken into account by using meson-pair exchanges (MPEs) (see below). Evidently, with cutoff masses $\Lambda \approx 1$ GeV, these form factors ensure a soft behavior of the potentials in configuration space at small distances. The form factors depend on the SU(3) assignment of the mesons, as described in detail in Ref. [9].

The potentials of the ESC model are generated by

(i) *One-boson-exchange (OBE).* The treatment of the OBE in the soft-core approach has been given for *NN* in Ref. [14], and for *YN* in Ref. [8]. With respect to these OBE interactions, the present ESC model contains, as mentioned above, two innovations. First, in the scalar meson form factor we have introduced a zero. This zero is natural in the $^3P_0$-pair-creation (QPC) [16–18] model for the coupling of the mesonic quark-antiquark ($Q\bar{Q}$) system to baryons. The scalar meson, being itself in this picture a $^3P_0$ $Q\bar{Q}$-bound state, gets a zero when it couples to a baryon. A pragmatic reason to exploit such a zero is that in this way we were able to avoid a bound state in ΛN scattering. Second, for the first time we incorporated axial-meson exchange into the potentials. As is well known, they are considered the chiral partners of the vector mesons. It turned out that the strength of the axial-meson exchanges is found to agree with the theoretical determination $g_{a_1} \approx (m_{a_1}/m_\pi) f_{NN\pi}$ [19,20].

(ii) *Two-meson-exchange (TME).* The configuration-space soft-core uncorrelated two-meson exchange for *NN* has been derived in Refs. [2,21]. We use these potentials in this paper for PS-PS exchange. Here, we give a complete SU(3)-symmetry treatment in *NN*, as well as in *YN* and *YY*. For example, we include double *K* exchange in *NN* scattering. Similarly, in papers II and III they are generalized to *YN* and *YY*, respectively. The PS-PS potentials contain the important long-range two-pion potentials. The other kind of two-meson exchanges such as pseudoscalar-vector (PS-V) and pseudoscalar-scalar (PS-S), are supposed to be less important because of cancellations and can be covered by OBE in an effective manner. Of course, this gives some contamination in the meson-baryon coupling constants.

(iii) *Meson-pair-exchange (MPE).* These exchanges been described for *NN* and justified in Ref. [3]. Again, in II and III the generalization is used in *YN* and *YY*. Also, the treatment given is complete as far as SU(3) is concerned. In Refs. [3,4] it is argued that the MPE potentials are thought to represent effects of heavy-meson exchange as well as meson-baryon resonances. Here we in particularly think about the πN resonances, like Δ_{33}.

A remarkable achievement with the ESC-model, in the version as described above, is that for the first time we could constrain the *NNM* couplings such that they are close to the predicted values of the QPC model. With the same parameters for the quark model, we find relations like $g_\epsilon \approx g_\omega \approx 3g_\rho \approx 3g_{a_0}$. Moreover, with the same $^3P_0$ parameters the predicted g_{a_1} agrees well with that of Ref. [19].

A particular new feature of these new ESC models is that we can allow for SU(3)-symmetry breaking of the coupling constants. In this breaking it is assumed that the amplitude for the creation of strange quarks from the vacuum is different than for nonstrange quarks. We consider this possibility explicitly in paper II, but in this paper we will assume, apart from meson mixing, no such SU(3) breaking.

The contents of this paper is as follows. In Sec. II we review the definition of the ESC potentials in the context of the relativistic two-body equations and the Thompson and Lippmann-Schwinger equations. Here we exploit the Macke-Klein [22] framework in field theory. For the Lippmann-Schwinger equation we introduce the usual potential forms in Pauli spinor space. We include here the central (C), the spin-spin (σ), the tensor (T), the spin-orbit (SO), the quadratic spin-orbit (Q_{12}), and the antisymmetric spin-orbit (ASO) potentials. For TME exchange, in the approximations made in Refs. [2,3] only the central, spin-spin, tensor, and spin-orbit potentials occur. In Sec. III the ESC potentials in momentum space are given, emphasizing the differences with earlier publications on the soft-core interactions. We discuss the OBE potentials, the PS-PS-interactions, and the MPE interactions. In Sec. IV we discuss the coupling constants from the point of view of the $^3P_0$ model. In Sec. V the *NN* results are displayed for coupling constants, scattering phases, low-energy parameters, and deuteron properties. Finally, in Sec. VI we give a general discussion and outlook.

Appendix contains the derivation of the axial-meson-exchange potentials.

II. TWO-BODY INTEGRAL EQUATIONS IN MOMENTUM SPACE

A. Relativistic two-body equations

We consider the nucleon-nucleon reactions

$$N(p_a, s_a) + N(p_b, s_b) \to N(p_{a'}, s_{a'}) + N(p_{b'}, s_{b'}) \quad (2.1)$$

with the total and relative four-momenta for the initial and the final states,

$$\begin{aligned} P &= p_a + p_b, & P' &= p_{a'} + p_{b'}, \\ p &= \tfrac{1}{2}(p_a - p_b), & p' &= \tfrac{1}{2}(p_{a'} - p_{b'}), \end{aligned} \quad (2.2)$$

which become in the center-of-mass system (c.m. system) for a and b on mass shell

$$P = (W, \mathbf{0}), \quad p = (0, \mathbf{p}), \quad p' = (0, \mathbf{p}'). \tag{2.3}$$

In general, the particles are off mass shell in the Green functions. In the remainder of this section, the on-mass-shell momenta for the initial and the final states are denoted, respectively, $\mathbf{p}$ and $\mathbf{p}'$. So, $p_a^0 = E_a(\mathbf{p}) = \sqrt{\mathbf{p}^2 + M_a^2}$ and $p_{a'}^0 = E_{a'}(\mathbf{p}') = \sqrt{\mathbf{p}'^2 + M_{a'}^2}$, and similarly for b and b'. Because of translation-invariance $P = P'$ and $W = W' = E_a(\mathbf{p}) + E_b(\mathbf{p}) = E_{a'}(\mathbf{p}') + E_{b'}(\mathbf{p}')$. The two-particle states we normalize in the following way:

$$\langle \mathbf{p}_1', \mathbf{p}_2' | \mathbf{p}_1, \mathbf{p}_2 \rangle = (2\pi)^3 2E(\mathbf{p}_1)\delta^3(\mathbf{p}_1' - \mathbf{p}_1) \times (2\pi)^3 2E(\mathbf{p}_2)\delta^3(\mathbf{p}_2' - \mathbf{p}_2). \tag{2.4}$$

The relativistic two-body scattering-equation for the scattering amplitude reads as [23–25]

$$M(p', p; P) = I(p', p; P) + \int d^4p''\, I(p', p''; P) \times G(p''; P) M(p'', p; P), \tag{2.5}$$

where $M(p', p; P)$ is a 16×16 matrix in Dirac space and the contributions to the kernel $I(p, p')$ come from the two-nucleon-irreducible Feynman diagrams. In writing Eq. (2.5) we have taken out an overall $\delta^4(P' - P)$ function, and the total four-momentum conservation is implicitly understood henceforth.

The two-baryon Green function $G(p; P)$ in Eq. (2.5) is simply the product of the free propagators for, in general, the baryons of the first and second lines. The baryon Feynman propagators are given by the well-known formula

$$G^{(s)}_{\{\mu\},\{\nu\}}(p) = \int d^4x \langle 0 | T\left(\psi^{(s)}_{\{\mu\}}(x)\bar{\psi}^{(s)}_{\{\nu\}}(0)\right)|0\rangle e^{ip\cdot x} = \frac{\Pi^s(p)}{p^2 - M^2 + i\delta}, \tag{2.6}$$

where $\psi^{(s)}_{\{\mu\}}$ is the free Rarita-Schwinger field that describes the nucleon ($s = \frac{1}{2}$), the Δ_{33}-resonance ($s = \frac{3}{2}$), etc. (see, for example Ref. [26]). For the nucleon, the only case considered in this paper, $\{\mu\} = \emptyset$ and for, e.g., the Δ resonance $\{\mu\} = \mu$. For the rest of this paper we deal only with nucleons.

In terms of these one-particle Green functions the two-particle Green function in Eq. (2.5) is

$$G(p; P) = \frac{i}{(2\pi)^4} \left[\frac{\Pi^{(s_a)}\left(\frac{1}{2}P + p\right)}{\left(\frac{1}{2}P + p\right)^2 - M_a^2 + i\delta} \right]^{(a)} \times \left[\frac{\Pi^{(s_b)}\left(\frac{1}{2}P - p\right)}{\left(\frac{1}{2}P - p\right)^2 - M_b^2 + i\delta} \right]^{(b)}. \tag{2.7}$$

Using now a complete set of on-mass-shell spin s states in the first line of Eq. (2.6) one finds that the Feynman propagator of a spin-s baryon off mass shell can be written as [27]

$$\frac{\Pi^{(s)}(p)}{p^2 - M^2 + i\delta} = \frac{M}{E(\mathbf{p})} \left[\frac{\Lambda_+^{(s)}(\mathbf{p})}{p_0 - E(\mathbf{p}) + i\delta} - \frac{\Lambda_-^{(s)}(-\mathbf{p})}{p_0 + E(\mathbf{p}) - i\delta} \right], \tag{2.8}$$

for $s = \frac{1}{2}, \frac{3}{2}, \ldots$. Here, $\Lambda_+^{(s)}(\mathbf{p})$ and $\Lambda_-^{(s)}(\mathbf{p})$ are the on-mass-shell projection operators on the positive- and negative-energy states. For the nucleon they are

$$\Lambda_+(\mathbf{p}) = \sum_{\sigma=-1/2}^{+1/2} u(\mathbf{p}, \sigma) \otimes \bar{u}(\mathbf{p}, \sigma), \qquad \Lambda_-(\mathbf{p}) = -\sum_{\sigma=-1/2}^{+1/2} v(\mathbf{p}, \sigma) \otimes \bar{v}(\mathbf{p}, \sigma), \tag{2.9}$$

where $u(\mathbf{p}, \sigma)$ and $v(\mathbf{p}, \sigma)$ are the Dirac spinors for spin-1/2 particles, and $E(\mathbf{p}) = \sqrt{\mathbf{p}^2 + M^2}$, with M the nucleon mass. Then, in the c.m. system, where $\mathbf{P} = 0$ and $P_0 = W$, the Green function can be written as

$$G(p; W) = \frac{i}{(2\pi)^4} \left(\frac{M_a}{E_a(\mathbf{p})}\right) \left[\frac{\Lambda_+^{(s_a)}(\mathbf{p})}{\frac{1}{2}W + p_0 - E_a(\mathbf{p}) + i\delta} - \frac{\Lambda_-^{(s_a)}(-\mathbf{p})}{\frac{1}{2}W + p_0 + E_a(\mathbf{p}) - i\delta} \right] \left(\frac{M_b}{E_b(\mathbf{p})}\right) \times \left[\frac{\Lambda_+^{(s_b)}(-\mathbf{p})}{\frac{1}{2}W - p_0 - E_b(\mathbf{p}) + i\delta} - \frac{\Lambda_-^{(s_b)}(\mathbf{p})}{\frac{1}{2}W - p_0 + E_b(\mathbf{p}) - i\delta} \right]. \tag{2.10}$$

Multiplying out Eq. (2.10), we write the ensuing terms in shorthand notation:

$$G(p; W) = G_{++}(p; W) + G_{+-}(p; W) + G_{-+}(p; W) + G_{--}(p; W), \tag{2.11}$$

where G_{++} etc. corresponds to the term with $\Lambda_+^{s_a}\Lambda_+^{s_b}$ etc. Introducing the spinorial amplitudes

$$M_{r's';rs}(p', p; P) = \bar{u}^{r'}(p_a', s_a')\bar{u}^{s'}(p_b', s_b')M(p', p; P) \times u^r(p_a, s_a)u^s(p_b, s_b), \quad (r, s = +, -), \tag{2.12}$$

with $(r, s) = +$ for the positive-energy Dirac spinors and $(r, s) = -$ for the negative-energy ones. Then, the two-body equation (2.5) for the spinorial amplitudes becomes

$$M_{r's';rs}(p', p; P) = I_{r's';rs}(p', p; P) + \sum_{r'',s''} \int d^4p'' I_{r's';r''s''}(p', p''; P) \times G_{r''s''}(p''; P) M_{r''s'';rs}(p'', p; P). \tag{2.13}$$

Invoking dynamical pair suppression, as discussed in Ref. [21], Eq. (2.13) reduces to a 4×4-dimensional equation

for $M_{++;++}$, i.e.,

$$M_{++;++}(p', p; P) = I_{++;++}(p', p; P) + \int d^4p''\ I_{++;++}(p', p''; P) \times G_{++}(p''; P) M_{++;++}(p'', p; P), \tag{2.14}$$

with the Green function

$$G_{++}(p; W) = \frac{i}{(2\pi)^4}\left[\frac{M_a M_b}{E_a(\mathbf{p}) E_b(\mathbf{p})}\right] \times \left[\frac{1}{2}W + p_0 - E_a(\mathbf{p}) + i\delta\right]^{-1} \times \left[\frac{1}{2}W - p_0 - E_b(\mathbf{p}) + i\delta\right]^{-1}. \tag{2.15}$$

B. Three-dimensional equation

In Ref. [21] we introduced starting from the Bethe-Salpeter equation for the two-baryon wave function $\psi(p^\mu)$ and applying the Macke-Klein procedure [22]. In this paper we employ the same procedure, but now for the two-baryon scattering amplitude $M(p', p; P)$. For any function $f(p_1, \ldots, p_n)$ we define the projection [28]

$$P_{R,p_i} f(p_1, \ldots, p_n) = f(p_1, \ldots, p_n) P_{L,i} \equiv \oint_{\mathrm{UHP}} dp_{i,0} A_W(p_i) f(\ldots, p_i, \ldots), \tag{2.16}$$

where the contour consists of the real axis and the infinite semicircle in the upper half-plane (UHP), and with Macke's right-inverse of the $\int dp_0$ operation

$$A_W(p) = (2\pi i)^{-1}\left(\frac{1}{p_0 + E_p - W - i\delta} + \frac{1}{-p_0 + E_p - W - i\delta}\right) = -\frac{1}{2\pi i}\frac{W - \mathcal{W}(\mathbf{p})}{F_W^{(a)}(\mathbf{p}, p_0) F_W^{(b)}(-\mathbf{p}, -p_0)}. \tag{2.17}$$

Here we used the frequently used notation

$$F_W(\mathbf{p}, p_0) = p_0 - E(\mathbf{p}) + \tfrac{1}{2}W + i\delta, \qquad \mathcal{W}(\mathbf{p}) = E_a(\mathbf{p}) + E_b(\mathbf{p}). \tag{2.18}$$

Notice that the Green function (2.15) can be written as

$$G_{++}(p; W) = \frac{1}{(2\pi)^3}\left[\frac{M_a M_b}{E_a(\mathbf{p}) E_b(\mathbf{p})}\right] \times A_W(p)\,(W - \mathcal{W}(p) + i\delta)^{-1}. \tag{2.19}$$

Now we make the rather solid assumption that for the scattering amplitudes the UHP contains no poles or branch points in the p_0 variable. Then one sees from Eq. (2.16) that as a result of the P_{R,p_i} operation the argument $p_{i0} \to W - E(\mathbf{p}_i)$, and similarly for P_{L,p_i}. Introducing the projections

$$P_{R,p'} M_{++;++}(p', p; P) P_{L,p} \equiv M(\mathbf{p}', \mathbf{p}|W), \tag{2.20a}$$

$$P_{R,p'} I_{++;++}(p', p; P) P_{L,p} \equiv K^{\mathrm{irr}}(\mathbf{p}', \mathbf{p}|W), \tag{2.20b}$$

we apply this to Eq. (2.14). This gives

$$M(\mathbf{p}', \mathbf{p}|W) = K^{\mathrm{irr}}(\mathbf{p}', \mathbf{p}|W) + \int \frac{d^3p''}{(2\pi)^3} \times \left[\frac{M_a M_b}{E_a(\mathbf{p}'') E_b(\mathbf{p}'')}\right](W - \mathcal{W}(\mathbf{p}'') + i\delta)^{-1} \times \left\{\int_{-\infty}^{\infty} dp_0'' I_{++;++}(p', p''; P)|_{p_0' = W - E(\mathbf{p}')} \times A_W(p'')\, M_{++;++}(p'', p; P)|_{p_0 = W - E(\mathbf{p})}\right\}. \tag{2.21}$$

Next, we redefine $M(\mathbf{p}'', \mathbf{p}|W)$ as

$$M(\mathbf{p}', \mathbf{p}|W) \to \sqrt{\frac{M_a M_b}{E_a(\mathbf{p}') E_b(\mathbf{p}')}}\, M(\mathbf{p}', \mathbf{p}|W) \sqrt{\frac{M_a M_b}{E_a(\mathbf{p}) E_b(\mathbf{p})}}, \tag{2.22}$$

and similarly for $K^{\mathrm{irr}}(\mathbf{p}'', \mathbf{p}|W)$. The thus redefined quantities again obey Eq. (2.21), except for the factor [. . .] on the right-hand side. Closing now the contour of the p_0'' integration in the upper half-plane, one again picks up only the contribution at $p_0'' = W - E(\mathbf{p}'')$, which means that Eq. (2.21) becomes the Thompson equation [29]:

$$M(\mathbf{p}', \mathbf{p}|W) = K^{\mathrm{irr}}(\mathbf{p}', \mathbf{p}|W) + \int \frac{d^3p''}{(2\pi)^3} K^{\mathrm{irr}} \times (\mathbf{p}', \mathbf{p}''|W) E_2^{(+)}(\mathbf{p}''; W) M(\mathbf{p}'', \mathbf{p}|W), \tag{2.23}$$

where $E_2^{(+)}(\mathbf{p}''; W) = (W - \mathcal{W}(\mathbf{p}'') + i\delta)^{-1}$. Written explicitly, we have from Eq. (2.20b) that the two-nucleon irreducible kernel is given by

$$K^{\mathrm{irr}}(\mathbf{p}', \mathbf{p}|W) = -\frac{1}{(2\pi)^2}\sqrt{\frac{M_a M_b}{E_a(\mathbf{p}') E_b(\mathbf{p}')}}\sqrt{\frac{M_a M_b}{E_a(\mathbf{p}) E_b(\mathbf{p})}} \times [W - \mathcal{W}(\mathbf{p}')][W - \mathcal{W}(\mathbf{p})] \times \int_{-\infty}^{+\infty} dp_0' \int_{-\infty}^{+\infty} dp_0 \Big\{\big[F_W^{(a)}(\mathbf{p}', p_0') \times F_W^{(b)}(-\mathbf{p}', -p_0')\big]^{-1} [I(p_0', \mathbf{p}'; p_0, \mathbf{p})]_{++,++} \times \big[F_W^{(a)}(\mathbf{p}, p_0) F_W^{(b)}(-\mathbf{p}, -p_0)\big]^{-1}\Big\}, \tag{2.24}$$

which is the same expression that we exploited in our previous papers, e.g., Refs. [2,5,21]. In the latter we exploited the three-dimensional wave function according to Salpeter [30] combined with the Macke-Klein ansatz [22]. For the scattering amplitude the derivation given above is more direct. For a discussion and comparison with other three-dimensional reductions of the Bethe-Salpeter equation we refer to Ref. [28]. In case one does not assume strong pair suppression, one must study instead of Eq. (2.14) a more general equation with couplings between the positive and the negative-energy

spinorial amplitudes. Also, to this more general case one can apply the described three-dimensional reduction, and we refer the reader to Ref. [28] for a treatment of this case.

The M/E factors in Eq. (2.24) are due to the difference between the relativistic and the nonrelativistic normalization of the two-particle states. In the following we simply put $M/E(\mathbf{p}) = 1$ in the kernel $K^{\rm irr}$, Eq. (2.24). The corrections to this approximation would give $(1/M)^2$ corrections to the potentials, which we neglect in this paper. In the same approximation there is no difference between the Thompson [29] and the Lippmann-Schwinger equations when the connection between these equations is made by using multiplication factors. Henceforth, we will not distinguish between the two.

The contributions to the two-particle irreducible kernel $K^{\rm irr}$ up to second order in the meson exchange are given in detail in Refs. [2,3].

C. Lippmann-Schwinger equation

The transformation of Eq. (2.23) to the Lippmann-Schwinger equation can be effectuated by defining

$$T(\mathbf{p}', \mathbf{p}) = N(\mathbf{p}')M(\mathbf{p}', \mathbf{p}|W)N(\mathbf{p}), \tag{2.25a}$$

$$V(\mathbf{p}', \mathbf{p}) = N(\mathbf{p}')K^{\rm irr}(\mathbf{p}', \mathbf{p}|W)N(\mathbf{p}), \tag{2.25b}$$

where the transformation function is

$$N(\mathbf{p}) = \sqrt{\frac{\mathbf{p}_i^2 - \mathbf{p}^2}{2M_N[E(\mathbf{p}_i) - E(\mathbf{p})]}}. \tag{2.26}$$

Application of this transformation yields the Lippmann-Schwinger equation,

$$T(\mathbf{p}', \mathbf{p}) = V(\mathbf{p}', \mathbf{p}) + \int \frac{d^3p''}{(2\pi)^3} \times V(\mathbf{p}', \mathbf{p}'')g(\mathbf{p}''; W)\, T(\mathbf{p}'', \mathbf{p}) \tag{2.27}$$

with the standard Green function

$$g(\mathbf{p}; W) = \frac{M_N}{\mathbf{p}_i^2 - \mathbf{p}^2 + i\delta}. \tag{2.28}$$

The corrections to the approximation $E_2^{(+)} \approx g(\mathbf{p}; W)$ are of order $1/M^2$, which we neglect hencforth.

The transition from Dirac spinors to Pauli spinors is given in Appendix C of Ref. [21], where we write for the the Lippmann-Schwinger equation in the four-dimensional Pauli-spinor space

$$\mathcal{T}(\mathbf{p}', \mathbf{p}) = \mathcal{V}(\mathbf{p}', \mathbf{p}) + \int \frac{d^3p''}{(2\pi)^3} \times \mathcal{V}(\mathbf{p}', \mathbf{p}'')g(\mathbf{p}''; W)\mathcal{T}(\mathbf{p}'', \mathbf{p}). \tag{2.29}$$

The $\mathcal{T}$ operator in Pauli spinor space is defined by

$$\chi^{(a)\dagger}_{\sigma_a'}\chi^{(b)\dagger}_{\sigma_b'}\, \mathcal{T}(\mathbf{p}', \mathbf{p})\, \chi^{(a)}_{\sigma_a}\chi^{(b)}_{\sigma_b} = \bar{u}_a(\mathbf{p}', \sigma_a')\bar{u}_b(-\mathbf{p}', \sigma_b') \times \tilde{T}(\mathbf{p}', \mathbf{p})\, u_a(\mathbf{p}, \sigma_a)u_b(-\mathbf{p}, \sigma_b), \tag{2.30}$$

and similarly for the $\mathcal{V}$ operator. As in the derivation of the OBE potentials [14,31], we make off shell and on shell the approximations $E(\mathbf{p}) = M + \mathbf{p}^2/2M$ and $W = 2\sqrt{\mathbf{p}_i^2 + M^2} = 2M + \mathbf{p}_i^2/M$ everywhere in the interaction kernels, which, of course, is fully justified only for low energies. In contrast to these kind of approximations, of course, the full $\mathbf{k}^2$ dependence of the form factors is kept throughout the derivation of the TME. Notice that the Gaussian form factors suppress the high-momentum transfers strongly. This means that the contribution to the potentials from intermediate states that are far off energy shell can not be very large.

Because of rotational invariance and parity conservation, the $\mathcal{T}$ and matrix, which is a 4×4 matrix in Pauli-spinor space, can be expanded into the following set of, in general, eight spinor invariants; see for example Ref. [32]. Introducing [33]

$$\mathbf{q} = \tfrac{1}{2}(\mathbf{p}' + \mathbf{p}), \quad \mathbf{k} = \mathbf{p}' - \mathbf{p}, \quad \mathbf{n} = \mathbf{p} \times \mathbf{p}', \tag{2.31}$$

with, of course, $\mathbf{n} = \mathbf{q} \times \mathbf{k}$, we choose for the operators P_j in spin space

$$P_1 = 1, \tag{2.32a}$$

$$P_2 = \boldsymbol{\sigma}_1 \cdot \boldsymbol{\sigma}_2, \tag{2.32b}$$

$$P_3 = (\boldsymbol{\sigma}_1 \cdot \mathbf{k})(\boldsymbol{\sigma}_2 \cdot \mathbf{k}) - \frac{1}{3}(\boldsymbol{\sigma}_1 \cdot \boldsymbol{\sigma}_2)\mathbf{k}^2, \tag{2.32c}$$

$$P_4 = \frac{i}{2}(\boldsymbol{\sigma}_1 + \boldsymbol{\sigma}_2) \cdot \mathbf{n}, \tag{2.32d}$$

$$P_5 = (\boldsymbol{\sigma}_1 \cdot \mathbf{n})(\boldsymbol{\sigma}_2 \cdot \mathbf{n}), \tag{2.32e}$$

$$P_6 = \frac{i}{2}(\boldsymbol{\sigma}_1 - \boldsymbol{\sigma}_2) \cdot \mathbf{n}, \tag{2.32f}$$

$$P_7 = (\boldsymbol{\sigma}_1 \cdot \mathbf{q})(\boldsymbol{\sigma}_2 \cdot \mathbf{k}) + (\boldsymbol{\sigma}_1 \cdot \mathbf{k})(\boldsymbol{\sigma}_2 \cdot \mathbf{q}), \tag{2.32g}$$

$$P_8 = (\boldsymbol{\sigma}_1 \cdot \mathbf{q})(\boldsymbol{\sigma}_2 \cdot \mathbf{k}) - (\boldsymbol{\sigma}_1 \cdot \mathbf{k})(\boldsymbol{\sigma}_2 \cdot \mathbf{q}). \tag{2.32h}$$

Here we follow Ref. [8], where in contrast to Ref. [14], we have chosen P_3 to be a purely tensor-force operator. The expansion in spinor invariants reads as

$$\mathcal{T}(\mathbf{p}', \mathbf{p}) = \sum_{j=1}^{8} \widetilde{T}_j(\mathbf{p}'^2, \mathbf{p}^2, \mathbf{p}' \cdot \mathbf{p})P_j(\mathbf{p}', \mathbf{p}). \tag{2.33}$$

Similarly to in Eq. (2.33), we expand the potentials V. Again following Eq. [8], we neglect the potential forms P_7 and P_8 and also the dependence of the potentials on $\mathbf{k} \cdot \mathbf{q}$. Then the expansion (2.33) reads for the potentials as follows:

$$\mathcal{V} = \sum_{j=1}^{4} \tilde{V}_j(\mathbf{k}^2, \mathbf{q}^2)P_j(\mathbf{k}, \mathbf{q}). \tag{2.34}$$

III. EXTENDED-SOFT-CORE POTENTIALS IN MOMENTUM SPACE

The potential of the ESC model contains the contributions from (i) one-boson exchanges, Fig. 1, (ii) uncorrelated two-pseudoscalar-exchange, Fig. 2 and Fig. 3, and (iii) meson-pair-exchange, Fig 4. In this section we review the potentials and indicate the changes with respect to earlier papers on the OBE and ESC models.

A. One-boson-exchange interactions in momentum space

The OBE potentials are the same as given in Refs. [8,14], with the exception of (i) the zero in the scalar form factor

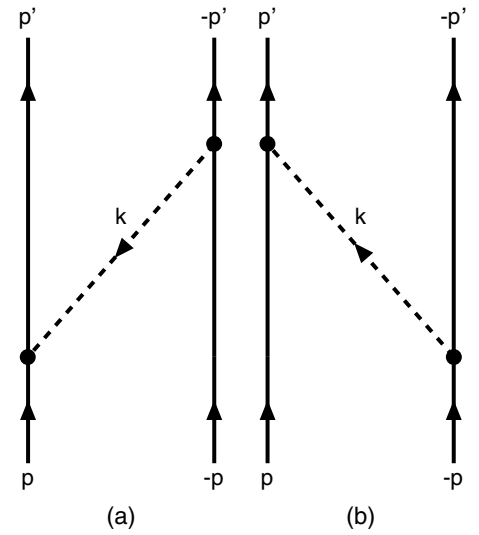

FIG. 1. One-boson-exchange graphs: the dashed lines with momentum **k** refers to the bosons: pseudoscalar, vector, axial-vector, or scalar mesons.

and (ii) the axial-vector-meson potentials. Here we review the OBE potentials briefly and give those potentials that are not incuded in the above references. The local interaction Hamilton densities for the various couplings follow:

(i) Pseudoscalar-meson exchange,

$$\mathcal{H}_{PV} = i\frac{f_P}{m_{\pi^+}}\bar{\psi}\gamma_\mu\gamma_5\psi\partial^\mu\phi_P, \tag{3.1}$$

(ii) Vector-meson exchange,

$$\mathcal{H}_V = ig_V\bar{\psi}\gamma_\mu\psi\phi_V^\mu + \frac{f_V}{4\mathcal{M}}\bar{\psi}\sigma_{\mu\nu}\psi\left(\partial^\mu\phi_V^\nu - \partial^\nu\phi_V^\mu\right). \tag{3.2}$$

(iii) Axial-vector-meson exchange,

$$\mathcal{H}_A = g_A\bar{\psi}\gamma_\mu\gamma_5\psi\phi_A^\mu + \frac{if_A}{\mathcal{M}}[\bar{\psi}\gamma_5\psi]\partial_\mu\phi_A^\mu. \tag{3.3}$$

We take $f_A = 0$ and notice that for the A_1 meson interaction (3.3) is part of the interaction

$$\mathcal{L}_I^{(A)} = 2g_A\left[\bar{\psi}\gamma_5\gamma_\mu\frac{\boldsymbol{\tau}}{2}\psi + (\boldsymbol{\pi}\partial_\mu\sigma - \sigma\partial_\mu\boldsymbol{\pi}) + f_\pi\partial_\mu\boldsymbol{\pi}\right]\cdot\mathbf{A}^\mu, \tag{3.4}$$

which is such that the A_1 couples to an almost conserved axial current (PCAC). Therefore the A_1 coupling used is compatible with broken $\mathrm{SU}(2)_V \times \mathrm{SU}(2)_A$ symmetry [20].

(iv) Scalar-meson exchange

$$\mathcal{H}_S = g_S\bar{\psi}\psi\phi_S. \tag{3.5}$$

Here, we used the conventions of Ref. [27], where $\sigma_{\mu\nu} = [\gamma_\mu, \gamma_\nu]/2i$. The scaling masses m_{π^+} and $\mathcal{M}$ are chosen to be the charged pion and the proton mass, respectively. Note that the vertices for diffractive exchange have the same Lorentz structure as those for scalar-meson exchange.

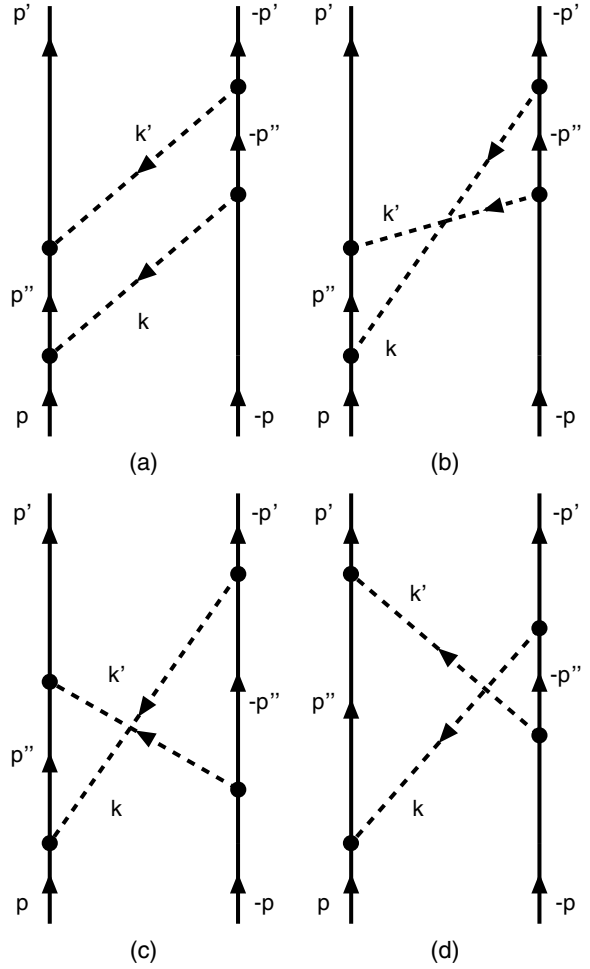

FIG. 2. BW two-meson-exchange graphs: (a) planar and (b)–(d) crossed box. The dashed line with momentum **k** refers to the pion, and the dashed line with momentum $\mathbf{k}'$ refers to one of the other (vector, scalar, or pseudoscalar) mesons. To these we have to add the mirror graphs and the graphs where we interchange the two meson lines.

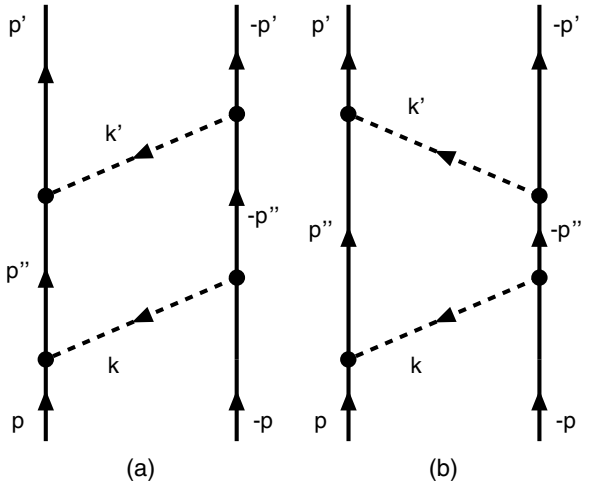

FIG. 3. Planar-box TMO two-meson-exchange graphs. Same notation as in Fig. 2. To these we have to add the mirror graphs and the graphs where we interchange the two meson lines.

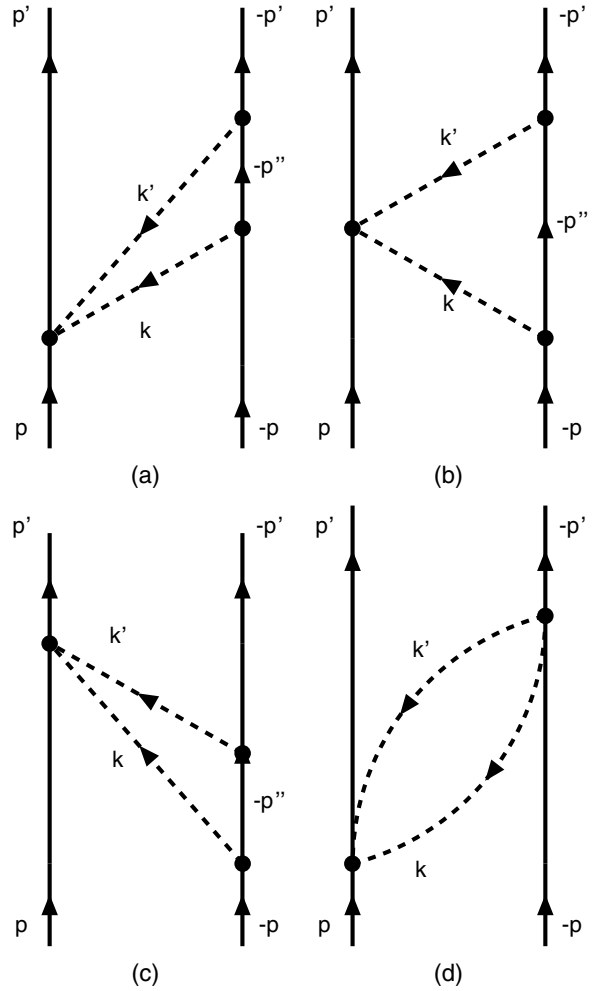

FIG. 4. One- and two-pair exchange graphs. To these we have to add the mirror graphs and the graphs where we interchange the two meson lines.

Including form factors $f(\mathbf{x}' - \mathbf{x})$, the interaction Hamiltonian densities are modified to

$$H_X(\mathbf{x}) = \int d^3x' f(\mathbf{x}' - \mathbf{x}) \mathcal{H}_X(\mathbf{x}') \tag{3.6}$$

for $X = PV, V, A, S$, or D. Because of the convolutive nonlocal form, the potentials in momentum space are the same as for point interactions, except that the coupling constants are multiplied by the Fourier transform of the form factors.

In the derivation of the V_i we employ the same approximations as in Refs. [8,14], i.e.,

(i) We expand in $1/M$: $E(p) = [\mathbf{k}^2/4 + \mathbf{q}^2 + M^2]^{1/2} \approx M + \mathbf{k}^2/8M + \mathbf{q}^2/2M$ and keep only terms up to first order in $\mathbf{k}^2/M$ and $\mathbf{q}^2/M$, except for the form factors, where the full $\mathbf{k}^2$ dependence is kept throughout the calculations. Notice that the Gaussian form factors suppress the high $\mathbf{k}^2$ contributions strongly.

(ii) In the meson propagators $[-(p_1 - p_3)^2 + m^2] \approx (\mathbf{k}^2 + m^2)$.

(iii) When two different baryons are involved at a BBM-vertex their average mass is used in the potentials, and the nonzero component of the momentum transfer is accounted for by using an effective mass in the meson propagator (for details see Ref. [8]).

Due to the approximations, we get only a linear dependence on $\mathbf{q}^2$ for V_1. In the following we write

$$V_i(\mathbf{k}^2, \mathbf{q}^2) = V_{ia}(\mathbf{k}^2) + V_{ib}(\mathbf{k}^2)\mathbf{q}^2, \tag{3.7}$$

where in principle $i = 1, 8$.

The OBE potentials are now obtained in the standard way (see e.g., Refs. [8,14]) by evaluating the BB interaction in the Born approximation. We write the potentials V_i of Eqs. (2.34) and (3.7) in the form

$$V_i(\mathbf{k}^2, \mathbf{q}^2) = \sum_X \Omega_i^{(X)}(\mathbf{k}^2) \cdot \Delta^{(X)}(\mathbf{k}^2, m^2, \Lambda^2), \tag{3.8}$$

where $X = P, V, A, S$, and D ($P =$ pseudoscalar, $V =$ vector, $A =$ axial-vector, $S =$ scalar, and $D =$ diffractive). Furthermore for $X = P, V$

$$\Delta^{(X)}(\mathbf{k}^2, m^2, \Lambda^2) = e^{-\mathbf{k}^2/\Lambda^2}/(\mathbf{k}^2 + m^2), \tag{3.9}$$

and for $X = S, A$ a zero in the form factor

$$\Delta^{(S)}(\mathbf{k}^2, m^2, \Lambda^2) = (1 - \mathbf{k}^2/U^2)e^{-\mathbf{k}^2/\Lambda^2}/(\mathbf{k}^2 + m^2), \tag{3.10}$$

and for $X = D$

$$\Delta^{(D)}(\mathbf{k}^2, m^2, \Lambda^2) = \frac{1}{\mathcal{M}^2} e^{-\mathbf{k}^2/(4m_P^2)}. \tag{3.11}$$

In the latter expression $\mathcal{M}$ is a universal scaling mass, which is again taken to be the proton mass. The mass parameter m_P controls the $\mathbf{k}^2$ dependence of the pomeron-, f-, f'-, A_2-, and $K^{\star\star}$-potentials.

Next, we point out the differences in the potentials of this work as compared with earlier soft-core model papers.

(i) For pseudoscalar mesons, the graphs of Fig. 1 give for the second-order potential $V_{PS}(\mathbf{k}, \mathbf{q}) \approx K_{PS}^{(2)}(\mathbf{p}', \mathbf{p}|W)$,

$$V_{PS}(\mathbf{k}, \mathbf{q}) = -\frac{f_{13} f_{24}}{m_\pi^2} \left[1 - \frac{(\mathbf{q}^2 + \mathbf{k}^2/4)}{2M_Y M_N}\right] \times \frac{(\boldsymbol{\sigma}_1 \cdot \mathbf{k})(\boldsymbol{\sigma}_2 \cdot \mathbf{k})}{\omega(\mathbf{k})[\omega(\mathbf{k}) + a]} \exp(-\mathbf{k}^2/\Lambda^2), \tag{3.12}$$

where $a \approx (\mathbf{q}^2 + \mathbf{k}^2/4) - p_i^2$. Here, p_i is the on-energy-shell momentum. On energy shell $a = 0$, and henceforth we neglect the nonadiabatic effects, i.e., $a \neq 0$, in the OBE potentials. However, we do include the nonlocal term in Eq. (3.12), to which we refer in the following as the Graz-correction [34]. From Eq. (3.12) we find for $\Omega_i^{(P)}$

$$\Omega_{2a}^{(P)} = g_{13}^P g_{24}^P \left(\frac{\mathbf{k}^2}{12 M_Y M_N}\right), \tag{3.13a}$$

$$\Omega_{2b}^{(P)} = -g_{13}^P g_{24}^P \left(\frac{\mathbf{k}^2}{24 M_Y^2 M_N^2}\right), \tag{3.13b}$$

$$\Omega_{3a}^{(P)} = -g_{13}^P g_{24}^P \left(\frac{1}{4 M_Y M_N}\right), \tag{3.13c}$$

$$\Omega_{3a}^{(P)} = +g_{13}^P g_{24}^P \left(\frac{1}{8 M_Y^2 M_N^2}\right). \tag{3.13d}$$

The $\Omega^{(P)}_{2b,3b}$ contributions were not included in Refs. [8,14].

(ii) For vector and diffractive OBE exchange we refer the reader to Ref. [8], where the contributions to the different $\Omega^{(X)}_i$'s for baryon-baryon scattering are given in detail. Also, it is trivial to obtain from Ref. [8] the scalar meson Ω_i, making the substitutions

$$\Omega^{(S)}_i \to (1-\mathbf{k}^2/U^2)\Omega^{(S)}_i$$

which now evidently have a zero for $\mathbf{k}^2 = U^2$.

(iii) For the axial-vector mesons, the detailed derivation of $\Omega^{(A)}_i$ is given in Appendix. Using approximations (1)–(5), from the first term in the axial-meson propagator, we get [see Eq. (A11)] the following contributions:

$$\Omega^{(A)}_{2a} = -g^A_{13}g^A_{24}\left(1+\frac{\mathbf{k}^2}{24M_YM_N}\right), \tag{3.14a}$$

$$\Omega^{(A)}_{2b} = -g^A_{13}g^A_{24}\frac{1}{6M_YM_N}, \tag{3.14b}$$

$$\Omega^{(A)}_{3} = +g^A_{13}g^A_{24}\frac{3}{4M_YM_N}, \tag{3.14c}$$

$$\Omega^{(A)}_{4} = -g^A_{13}g^A_{24}\frac{1}{2M_YM_N}, \tag{3.14d}$$

$$\Omega^{(A)}_{6} = -g^A_{13}g^A_{24}\frac{M_N^2-M_Y^2}{4M_Y^2M_N^2}. \tag{3.14e}$$

From the second-term propagator we get [see Eq. (A13)]

$$\Omega^{(A)}_{2a} = -g^A_{13}g^A_{24}\left(1-\frac{\mathbf{k}^2}{8M_YM_N}\right)\cdot\frac{\mathbf{k}^2}{3m^2}, \tag{3.15a}$$

$$\Omega^{(A)}_{2b} = +g^A_{13}g^A_{24}\frac{1}{2M_YM_N}\cdot\frac{\mathbf{k}^2}{3m^2}, \tag{3.15b}$$

$$\Omega^{(A)}_{3a} = -g^A_{13}g^A_{24}\left(1-\frac{\mathbf{k}^2}{8M_YM_N}\right)\cdot\frac{1}{m^2}, \tag{3.15c}$$

$$\Omega^{(A)}_{3b} = +g^A_{13}g^A_{24}\frac{1}{2M_YM_N}\cdot\frac{1}{m^2}. \tag{3.15d}$$

For the inclusion of the zero in the axial-vector meson form factor here we also make the changes

$$\Omega^{(A)}_i \to (1-\mathbf{k}^2/U^2)\Omega^{(A)}_i$$

with the same U mass as used for the scalar mesons. The inclusion of a zero in the form factor here is again motivated by the quark model, because for the axial-vector mesons one has the configuration $Q\bar{Q}(^3P_1)$.

As in Ref. [8] in the derivation of the expressions for $\Omega^{(A)}_i$, given above, M_Y and M_N denote the mean hyperon and nucleon mass, respectively, $M_Y = (M_1+M_3)/2$ and $M_N = (M_2+M_4)/2$, and m denotes the mass of the exchanged meson. Moreover, the approximation $1/M_N^2 + 1/M_Y^2 \approx 2/M_NM_Y$ is used, which is rather good, since the mass differences between the baryons are not large.

B. One-boson-exchange interactions in configuration space

(i) For $X = P$ the local configuration-space potentials are given in Ref. [8]. Here, we give the nonlocal Graz corrections. From the Fourier transform of the $\Omega^{(P)}_{2b,3b}$ contributions and Eq. (3.13d) we have

$$\Delta V_{PS}(r) = \frac{f_{13}f_{24}}{4\pi}\cdot\frac{m^3}{m_\pi^2}\cdot\Big[\frac{1}{3}(\boldsymbol{\sigma}_1\cdot\boldsymbol{\sigma}_2)\left(\nabla^2\phi^1_C+\phi^1_C\nabla^2\right) + \left(\nabla^2\phi^0_T S_{12}+\phi^0_T S_{12}\nabla^2\right)\Big]\Big/(4M_YM_N), \tag{3.16}$$

where $\phi^0_C, \phi^1_C, \phi^0_T$ are defined in Refs. [8,14] and are functions of (m, r, Λ).

(ii) Again, for $X = V, D$ we refer to the configuration-space potentials in Ref. [8]. For $X = S$ we give here the additional terms with respect to those in Ref. [8], which are due to the zero in the scalar form factor. They are

$$\Delta V_S(r) = -\frac{m}{4\pi}\frac{m^2}{U^2}\Big\{g^S_{13}g^S_{24}\Big[\Big(\phi^1_C-\frac{m^2}{4M_YM_N}\phi^2_C\Big) + \frac{m^2}{2M_YM_N}\phi^1_{\rm SO}\mathbf{L}\cdot\mathbf{S}+\frac{m^4}{16M_Y^2M_N^2}\phi^1_T Q_{12} + \frac{m^2}{4M_YM_N}\frac{M_N^2-M_Y^2}{M_YM_N}\phi^{(1)}_{\rm SO}\cdot\frac{1}{2}(\boldsymbol{\sigma}_1-\boldsymbol{\sigma}_2)\cdot\mathbf{L}\Big]\Big\}. \tag{3.17}$$

(iii) For the axial-vector mesons, the configuration-space potential corresponding to Eq. (3.14e) is

$$V^{(1)}_A(r) = -\frac{g_A^2}{4\pi}m\Big[\phi^0_C(\boldsymbol{\sigma}_1\cdot\boldsymbol{\sigma}_2)-\frac{1}{12M_YM_N} \times\left(\nabla^2\phi^0_C+\phi^0_C\nabla^2\right)(\boldsymbol{\sigma}_1\cdot\boldsymbol{\sigma}_2)+\frac{3m^2}{4M_YM_N}\phi^0_T S_{12} + \frac{m^2}{2M_YM_N}\phi^0_{\rm SO}(m,r)\mathbf{L}\cdot\mathbf{S}+\frac{m^2}{4M_YM_N} \times\frac{M_N^2-M_Y^2}{M_YM_N}\phi^{(0)}_{\rm SO}\cdot\frac{1}{2}(\boldsymbol{\sigma}_1-\boldsymbol{\sigma}_2)\cdot\mathbf{L}\Big]. \tag{3.18}$$

The configuration-space potential corresponding to Eq. (3.15d) is

$$V^{(2)}_A(r) = \frac{g_A^2}{4\pi}m\Big[\frac{1}{3}(\boldsymbol{\sigma}_1\cdot\boldsymbol{\sigma}_2)\phi^1_C+\frac{1}{12M_YM_N}(\boldsymbol{\sigma}_1\cdot\boldsymbol{\sigma}_2) \times\left(\nabla^2\phi^1_C+\phi^1_C\nabla^2\right)+S_{12}\phi^0_T + \frac{1}{4M_YM_N}\left(\nabla^2\phi^0_T S_{12}+\phi^0_T S_{12}\nabla^2\right)\Big]. \tag{3.19}$$

The extra contribution to the potentials coming from the zero in the axial-vector meson form factor are obtained from expression (3.18) by making substitutions as follows:

$$\Delta V^{(1)}_A(r) = V^{(1)}_A\left(\phi^0_C\to\phi^1_C, \phi^0_T\to\phi^1_T, \phi^0_{\rm SO}\to\phi^1_{\rm SO}\right)\cdot\frac{m^2}{U^2}. \tag{3.20}$$

Note that we do not include the similar $\Delta V^{(2)}_A(r)$, since they involve $\mathbf{k}^4$ terms in momentum space.

C. *PS-PS*-exchange interactions in configuration space

In Figs. 2 and 3 the included two-meson exchange graphs are shown schematically. The Bruckner-Watson (BW) graphs [35] contain in all three intermediate states both mesons and nucleons. The Taketani-Machida-Ohnuma (TMO) graphs [36] have one intermediate state with only nucleons. Explicit expressions for $K^{\rm irr}$(BW) and $K^{\rm irr}$(TMO) were derived in Ref. [21], where the terminology BW and TMO is also explained. The TPS potentials for nucleon-nucleon pairs have been given in detail in Ref. [2]. The generalization to baryon-baryon pairs is similar to that for the OBE potentials. So, we substitute $M \to \sqrt{M_Y M_N}$, and include all *PS-PS* possibilities with coupling constants as in the OBE potentials. As compared with nucleon-nucleon pairs in Ref. [2], here we have included in addition the potentials with double K exchange. The masses are the physical pseudoscalar meson masses. For the intermediate two-baryon states we take into account the different thresholds. We have not included uncorrelated *PS*-vector, *PS*-scalar, or *PS*-diffractive exchange. This because the range of these potentials is similar to those of the vector, scalar, and axial-vector potentials. Moreover, for potentially large potentials, in particularly those with scalar mesons involved, there will be very strong cancellations between the planar and the crossed-box contributions.

D. MPE-exchange interactions

In Fig. 4 both the one-pair graphs and the two-pair graphs are shown. In this work we include only the one-pair graphs. The argument for neglecting the two-pair graph is to avoid some double-counting. Viewing the pair vertex as containing heavy-meson exchange means that the contributions from $\rho(750)$ and $\epsilon = f_0(760)$ to the two-pair graphs is already accounted for by our treatment of the broad ρ and ϵ OBE potential. For a more complete discussion of the physics behind MPE, we refer to our previous papers [1,3]. The MPE potentials for nucleon-nucleon pairs have been given in Ref. [3]. The generalization to baryon-baryon pairs is similar to that for the TPS potentials. For the intermediate two-baryon states we neglect the different two-baryon thresholds. This because, although in principle they are possible, they complicate the computation of the potentials considerably. The generalization of the pair couplings to baryon-baryon pairs is described in paper II [10], Sec. III. Also here in NN, we have in addition to [3] included the pair potentials with $K \otimes K$-, $K \otimes K^*$-, and $K \otimes \kappa$ exchange. The convention for the MPE coupling constants is the same as in Ref. [3].

E. Schrödinger equation with nonlocal potential

The nonlocal potentials are of the central-, spin-spin, and tensor type. The method of solution of the Schrödinger equation for nucleon-nucleon pairs is described in Ref. [14] and [34]. Here the nonlocal tensor is in momentum space of the form $\mathbf{q}^2 \tilde{v}_T(\mathbf{k})$. For a more general treatment of the nonlocal potentials, see Ref. [37].

IV. ESC COUPLINGS AND THE QPC MODEL

According to the quark-pair-creation (QPC) model, in the $^3P_0$ version [16], the baryon-baryon-meson couplings are given in terms of the quark-pair creation constant γ_M, and the radii of the (constituent) Gaussian quark wave functions by [17,18]

$$g_{\rm BBM}(\mp) = 2\,(9\pi)^{1/4}\,\gamma_M X_M\,(I_M, L_M, S_M, J_M)\,F_M^{(\mp)}$$

where $X_M(\ldots)$ is a isospin, spin, etc. recoupling coefficient and

$$F^{(-)} = (m_M R_M)^{3/2}\left(\frac{3R_B^2}{3R_B^2+R_M^2}\right)^{3/2}\left(\frac{4R_B^2+R_M^2}{3R_B^2+R_M^2}\right)$$

$$F^{(+)} = (m_M R_M)^{1/2}\left(\frac{3R_B^2}{3R_B^2+R_M^2}\right)^{3/2}\frac{4R_M^2}{(3R_B^2+R_M^2)},$$

are coming from the overlap integrals. Here, the superscripts $\mp$ refer to the parity of the mesons M: $(-)$ for $J^{\rm PC} = 0^{+-}, 1^{--}$, and $(+)$ for $J^{\rm PC} = 0^{++}, 1^{++}$. The radii of the baryons, in this case nucleons, and the mesons are respectively denoted by R_B and R_M.

The QPC($^3P_0$) model gives several interesting relations, such as

$$\begin{aligned} g_\omega &= 3g_\rho, \quad & g_\epsilon &= 3g_{a_0}, \\ g_{a_0} &\approx g_\rho, \quad & g_\epsilon &\approx g_\omega. \end{aligned} \tag{4.1}$$

We see here an interesting link between the vector-meson and the scalar-meson couplings, which is not totally surprising, because the scalar polarization vector ϵ_0 of the vector mesons in the quark model is realized by a $Q\bar{Q}(^3P_0)$ state. This is the same state as for the scalar mesons in the $Q\bar{Q}$ picture.

From $\rho \to e^+e^-$, employing the current field identities (C.F.I's) one can derive (see for example Ref. [38]) the following relation with the QPC model:

$$f_\rho = \frac{m_\rho^{3/2}}{\sqrt{2}|\psi_\rho(0)|} \Leftrightarrow \gamma_M \left(\frac{2}{3\pi}\right)^{1/2}\frac{m_\rho^{3/2}}{|'\psi_\rho(0)'|}, \tag{4.2}$$

which, neglecting the difference between the wave functions on the left- and right-hand sides, gives for the pair creation constant $\gamma_M \to \gamma_0 = \frac{1}{2}\sqrt{3\pi} = 1.535$. However, since in the QPC model Gaussian wave functions are used, the $Q\bar{Q}$ potential is a harmonic-oscillator one. This does not account for the $1/r$ behavior, due to one-gluon-exchange (OGE), at short distance. This implies a OG correction [39] to the wave function, which gives for γ_M [40]

$$\gamma_M = \gamma_0\left[1 - \frac{16}{3}\frac{\alpha(m_M)}{\pi}\right]^{-1/2}. \tag{4.3}$$

In Table I $\gamma_M(\mu)$ is shown, using from Ref. [41] the parametrization

$$\alpha_s(\mu) = 4\pi\big/\big[\beta_0 \ln\big(\mu^2\big/\Lambda_{\rm QCD}^2\big)\big], \tag{4.4}$$

with $\Lambda_{\rm QCD} = 100$ MeV and $\beta_0 = 11 - \frac{2}{3}n_f$ for $n_f = 3$.

From this table one sees that at the scale of $m_M \approx 1$ GeV a value $\gamma_M = 2.19$ is reasonable. This value we will use later when comparing the QPC-model predictions and the ESC04-model coupling constants. As remarked in Ref. [40],

TABLE I. Pair-creation constant γ_M as function of α_s.

μ [GeV]	$\alpha_s(\mu)$	$\gamma_M(\mu)$
∞	0.00	1.535
80.0	0.10	1.685
35.0	0.20	1.889
1.05	0.30	2.191
0.55	0.40	2.710
0.40	0.50	3.94
0.35	0.55	5.96

the correction to γ_0 is not small, and therefore should be seen as an indication.

In Table II we show the $^3P_0$-model results and the values obtained in the ESC04 fit. In this table we fixed $\gamma_M = 2.19$ for the vector, scalar, and axial-vector mesons, for $R_B = 0.54$ fm. This effective radius is choosen from Ref. [17], where it was determined by using the Regge slopes. Here, one has to realize that the QPC predictions are kind of bare couplings, which allows vertex corrections from meson exchange. For the pseudoscalar, a different value has to be used, showing indeed some running behavior as expected from QCD. In Ref. [40], for the decays $\rho, \epsilon \to 2\pi$, etc., was found $\gamma_\pi = 3.33$, whereas here we need $\gamma_\pi = 4.84$. Of course, there are several ways to change this by, for example, using other effective meson radii. For the mesonic decays of the charmonium states $\gamma_\psi = 1.12$, one notices the similarity between the QPC($^3P_0$)-model predictions and the fitted couplings.

Finally, we notice that the Schwinger relation [19]

$$g_{NNa_1} \approx \frac{m_{a_1}}{m_\pi} f_{NN\pi} \tag{4.5}$$

is also rather well satisfied, both in the QPC model and the ESC04 fit.

V. ESC-MODEL RESULTS

A. Parameters and nucleon-nucleon fit

During the searches fitting the *NN* data with the present ESC-model ESC04, it was found that the OBE couplings could be constrained successfully by using the naive QPC predictions as guidance [16]. Although these predictions (see Sec. IV) are bare ones, we kept during the searches all OBE couplings rather closely in the neighborhood of these predictions. Also, it appeared that we could either fix all $F/(F+D)$ ratios to those suggested by the QPC model or apply the same strategy as for the OBE couplings.

TABLE II. ESC04 couplings and $^3P_0$ model relations.

Meson	r_M[fm]	X_M	γ_M	$^3P_0$	ESC04
$\pi(140)$	0.66	5/6	4.84	$f = 0.26$	$f = 0.26$
$\rho(770)$	0.66	1	2.19	$g = 0.93$	$g = 0.78$
$\omega(783)$	0.66	3	2.19	$g = 2.86$	$g = 3.12$
$a_0(962)$	0.66	1	2.19	$g = 0.93$	$g = 0.81$
$\epsilon(760)$	0.66	3	2.19	$g = 2.47$	$g = 2.87$
$a_1(1270)$	0.66	$5\sqrt{2}/6$	2.19	$g = 2.51$	$g = 2.42$

The meson nonets contain rm SU(3) octet and mixed octet-singlet members. We assign in principle cutoffs Λ_8 and Λ_1 to the octets and singlets, respectively. However, because of the octet-singlet mixings for the $I = 0$ members, and the use of the physical mesons in the potentials, we use Λ_1 for all $I = 0$ mesons. We have as free cutoff parameters (Λ_8^P, Λ_8^V, Λ_8^S), and similarly a set for the singlets. For the axial-vector mesons we use a single cutoff Λ^A.

The treatment of the broad mesons ρ and ϵ is the same as in the OBE models [8,14]. In this treatment a broad meson is approximated by two narrow mesons. The mass and width of the broad meson determines the masses $m_{1,2}$ and the weights $\beta_{1,2}$ of these narrow ones. For the ρ meson the same parameters are used as in Refs. [8,14]. However, for $\epsilon = f_0(760)$, assuming [14]$m_\epsilon = 760$ MeV and $\Gamma_\epsilon = 640$ MeV, the Bryan-Gersten parameters [42] are used: $m_1 = 496.39796$ MeV, $m_2 = 1365.59411$ MeV, and $\beta_1 = 0.21781$, $\beta_2 = 0.78219$.

The mass of the diffractive exchanges were all fixed to $m_P = 309.1$ MeV.

Summarizing the parameters we have for *NN* are

(i) QPC constrained, $f_{NN\pi}, f_{NN\eta'}, g_{NN\rho}, g_{NN\omega}$, $f_{NN\rho}$, $f_{NN\omega}$, $g_{NNa_1}, g_{a_0}, g_{NN\epsilon}, g_{NNA_2}, g_{NNP}$;
(ii) Pair couplings, $g_{NN(\pi\pi)_1}, f_{NN(\pi\pi)_1}, g_{NN(\pi\rho)_1}$, $g_{NN\pi\omega}$, $g_{NN\pi\eta}, g_{NN\pi\epsilon}$;
(iii) Cutoff masses, $\Lambda_8^P, \Lambda_8^V, \Lambda_8^S, \Lambda_1^V, \Lambda_1^S, \Lambda^A$.

The pair coupling $g_{NN(\pi\pi)_0}$ was kept fixed at a small, but otherwise arbitrary value.

Together with the fit to the 1993 Nijmegen representation of the χ^2 hypersurface of the *NN*-scattering data below $T_{\rm lab} = 350$ MeV [43], also some low-energy parameters were also fitted: the *np* and *nn* scattering lengths and effective ranges for the $^1S_0$, and the binding energy of the deuteron E_B.

We obtained for the phase shifts $\chi^2/N_{\rm data} = 1.155$. The phase shifts are shown in Tables III and IV and also in Figs. 5–8. In Table VIII below the distribution of the χ^2 for ESC04 is shown for the ten energy bins used in the single-energy (s.e.) phase shift analysis and compared with that of the updated partial-wave analysis [45].

We emphasize that we use the single-energy (s.e.) phases and χ^2-surfaces [45] only as a means to fit the *NN* data. As stressed in Ref. [43] the Nijmegen s.e. phases have not much significance. The significant phases are the multienergy (m.e.) ones; see the dashed curves in the figures. One notices that the central value of the s.e. phases do not correspond to the m.e. phases in general, illustrating that there has been a certain amount of noise fitting in the s.e. partial wave (PW)-analysis; see, e.g., ϵ_1 and $^1P_1$ at $T_{\rm lab} = 100$ MeV. The m.e. PW analysis reaches $\chi^2/N_{\rm data} = 0.99$, using 39 phenomenological parameters plus normalization parameters, in total more than 50 free parameters. The related phenomenological PW potentials NijmI, II and Reid93 [46], have, respectively, 41, 47, and 50 parameters, all with $\chi^2/N_{\rm data} = 1.03$. This should be compared with the ESC model, which has $\chi^2/N_{\rm data} = 1.155$ for 20 parameters. These are 11 QPC-constrained meson-nucleon-nucleon couplings, 6 meson-pair-nucleon-nucleon

TABLE III. ESC04 *pp* and *np* nuclear-bar phase shifts in degrees.

	$T_{\rm lab}$				
	0.38	1	5	10	25
No. of data	144	68	103	290	352
$\Delta\chi^2$	20	38	17	34	12
$^1S_0(np)$	54.58	61.89	63.04	59.13	49.66
$^1S_0$	14.62	32.63	54.76	55.16	48.58
$^3S_1$	159.38	147.76	118.21	102.66	80.76
ϵ_1	0.03	0.11	0.67	1.14	1.72
$^3P_0$	0.02	0.13	1.55	3.67	8.50
$^3P_1$	−0.01	−0.08	−0.87	−1.98	−4.78
$^1P_1$	−0.05	−0.19	−1.52	−3.12	−6.49
$^3P_2$	0.00	0.01	0.22	0.66	2.49
ϵ_2	−0.00	−0.00	−0.05	−0.19	−0.78
$^3D_1$	0.00	−0.01	−0.19	−0.69	−2.85
$^3D_2$	0.00	0.01	0.22	0.86	3.73
$^1D_2$	0.00	0.00	0.04	0.16	0.68
$^3D_3$	0.00	0.00	0.00	0.00	0.04
ϵ_3	0.00	0.00	0.01	0.08	0.56
$^3F_2$	0.00	0.00	0.00	0.01	0.10
$^3F_3$	0.00	0.00	−0.00	−0.03	−0.22
$^1F_3$	0.00	0.00	−0.01	−0.07	−0.42
$^3F_4$	0.00	0.00	0.00	0.00	0.02
ϵ_4	0.00	0.00	0.00	−0.00	−0.05

TABLE IV. ESC04 *pp* and *np* nuclear-bar phase shifts in degrees.

	$T_{\rm lab}$				
	50	100	150	215	320
No. of data	572	399	676	756	954
$\Delta\chi^2$	118	29	114	137	337
$^1S_0(np)$	38.81	24.24	13.80	3.27	−9.80
$^1S_0$	38.77	24.71	14.42	3.97	−9.05
$^3S_1$	63.03	43.79	31.66	20.27	6.93
ϵ_1	1.96	2.18	2.50	3.08	4.21
$^3P_0$	11.51	9.68	5.14	−1.13	−10.19
$^3P_1$	−8.16	−13.22	−17.43	−22.24	−28.81
$^1P_1$	−9.92	−14.65	−18.67	−22.37	−29.87
$^3P_2$	5.78	10.94	14.09	16.26	17.28
ϵ_2	−1.66	−2.63	−2.92	−2.77	−2.13
$^3D_1$	−6.58	−12.67	−17.29	−21.90	−27.41
$^3D_2$	8.97	17.20	22.06	24.92	25.15
$^1D_2$	1.67	3.77	5.76	7.82	9.65
$^3D_3$	0.27	1.28	2.53	3.94	5.24
ϵ_3	1.62	3.52	4.87	6.01	6.93
$^3F_2$	0.32	0.75	1.00	0.97	0.07
$^3F_3$	−0.65	−1.42	−2.02	−2.65	−3.63
$^1F_3$	−1.12	−2.18	−2.87	−3.56	−4.70
$^3F_4$	0.11	0.46	0.95	1.67	2.84
ϵ_4	−0.19	−0.51	−0.81	−1.11	−1.44
$^3G_3$	−0.27	−0.99	−1.88	−3.10	−4.92
$^3G_4$	0.72	2.14	3.56	5.20	7.29
$^1G_4$	0.15	0.40	0.67	1.02	1.63
$^3G_5$	−0.05	−0.19	−0.32	−0.42	−0.43
ϵ_5	0.21	0.72	1.26	1.90	2.75

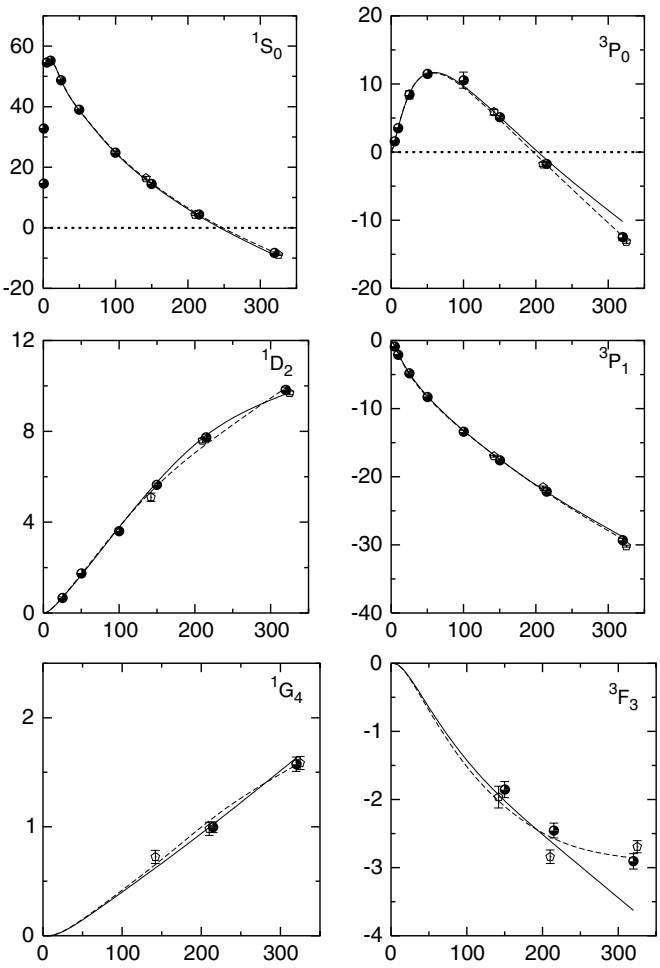

FIG. 5. Solid curves, proton-proton $I = 1$ phase shifts (degrees), as a function of $T_{\rm lab}$(MeV), for the ESC04 model. Dashed curves, the m.e. phases of the Nijmegen93 PW analysis [43]. Dots, s.e. phases of the Nijmegen93 PW analysis. Pentagons, Bugg s.e. [44].

couplings, and 3 Gaussian cutoff parameters. From the figures it is obvious that the ESC model deviates from the m.e. PW analysis at the highest energy for some partial waves. If we evaluate the χ^2 for the first 9 energies only, we obtain $\chi^2/N_{\rm data} = 1.10$.

In Table V the results for the low-energy parameters are given. In order to discriminate between the $^1S_0$ wave for *pp*, *np*, and *nn*, we introduced some charge independence breaking by taking $g_{pp\rho} \neq g_{np\rho} \neq g_{nn\rho}$. With this device we fitted the difference between the $^1S_0$ (*pp*) and $^1S_0$ (*np*) phases, and the different scattering lengths and effective ranges as well. We found $g_{np\rho} = 0.71$, $g_{nn\rho} = 0.74$, which are not far from $g_{pp\rho} = 0.78$; see Table VI.

For $a_{nn}(^1S_0)$ we have used in the fitting the value from an investigation of the *n-p* and *n-n* final state interaction in the ^{2}H(n, nnp) reaction at 13 MeV [47]. The value for $a_{nn}(^1S_0)$ is still somewhat under discussion. Another recent determination [48] obtained, e.g., $a_{nn}(^1S_0) = -16.27 \pm 0.40$ fm. Fitting with the latter value yields for the ESC04 model the value −16.74 fm. Then the quality of the fit to the phase shift analysis is the same, with small changes to the parameters and phase

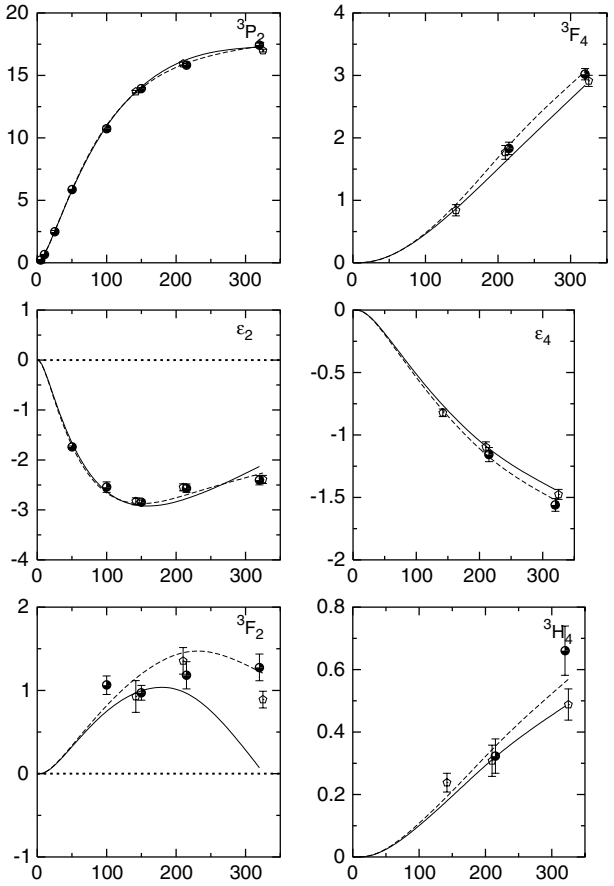

FIG. 6. Solid curves, proton-proton $I = 1$ phase shifts (degrees), as a function of $T_{\rm lab}$(MeV), for the ESC04 model. Dashed curves, m.e. phases of the Nijmegen93 PW analysis [43]. Dots, s.e. phases of the Nijmegen93 PW analysis. Pentagons, Bugg s.e. [44].

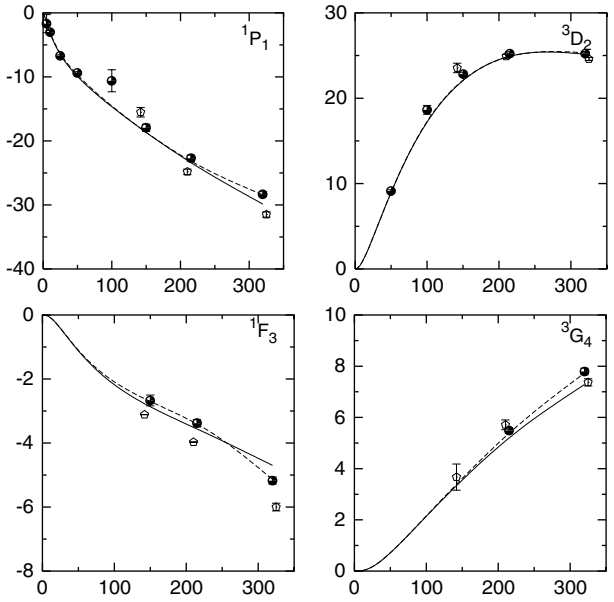

FIG. 7. Solid curves, neutron-proton $I = 0$ phase shifts (degrees), as a function of $T_{\rm lab}$(MeV) for the ESC04 model. Dashed curves, m.e. phases of the Nijmegen93 PW analysis [43]. Dots, s.e. phases of the Nijmegen93 PW analysis. Pentagons, Bugg s.e. [44].

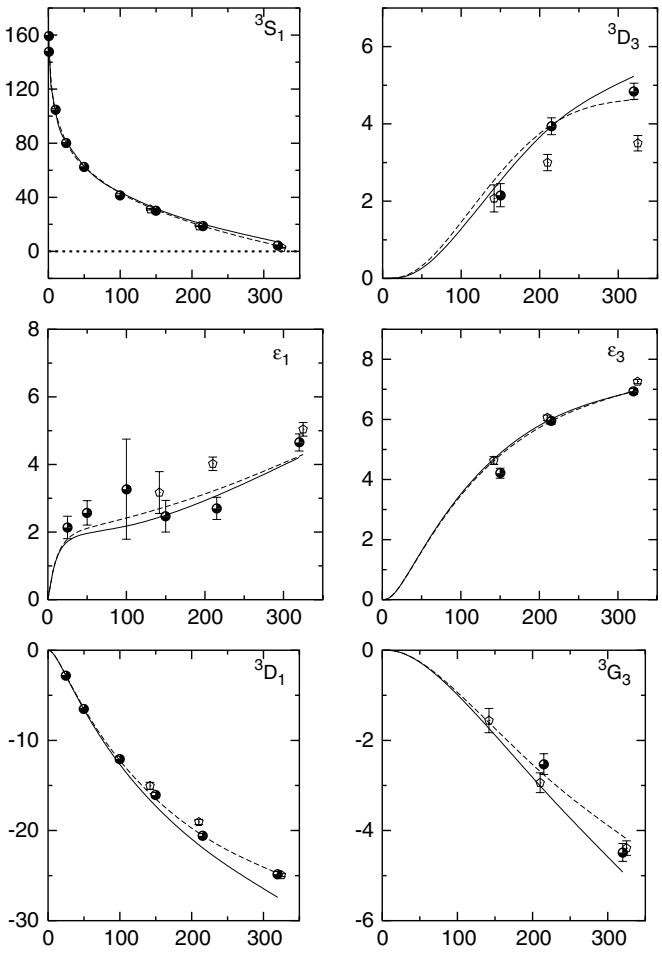

FIG. 8. Solid curves, neutron-proton $I = 0$ phase shifts (degrees), as a function of $T_{\rm lab}$(MeV) for the ESC04 model. Dashed curves, m.e. phases of the Nijmegen93 PW analysis [43]. Dots, s.e. phases of the Nijmegen93 PW analysis. Pentagons, Bugg s.e. [44].

shifts. For a discussion of the theoretical and experimental situation with respect to these low-energy parameters, see also Ref. [49].

TABLE V. ESC04 low-energy parameters: S-wave scattering lengths and effective ranges, deuteron binding energy E_B, and electric quadrupole Q_e.

	Experimental data	ESC04
$a_{pp}(^1S_0)$	-7.823 ± 0.010	-7.770
$r_{pp}(^1S_0)$	2.794 ± 0.015	2.753
$a_{np}(^1S_0)$	-23.715 ± 0.015	-23.860
$r_{np}(^1S_0)$	2.760 ± 0.030	2.787
$a_{nn}(^1S_0)$	-18.70 ± 0.60	-18.63
$r_{nn}(^1S_0)$	2.75 ± 0.11	2.81
$a_{np}(^3S_1)$	5.423 ± 0.005	5.404
$r_{np}(^3S_1)$	1.761 ± 0.005	1.749
E_B	-2.224644 ± 0.000046	-2.224933
Q_e	0.286 ± 0.002	0.271

TABLE VI. Meson parameters employed in the potentials shown in Figs. 1–4. Coupling constants are at $\mathbf{k}^2 = 0$. An asterisk denotes that the coupling constant is not searched, but constrained via SU(3) or simply set to some value used in previous work. The widths of ρ and ε used are 146 and 640 MeV, respectively.

Meson	Mass (MeV)	$g/\sqrt{4\pi}$	$f/\sqrt{4\pi}$	Λ (MeV)
π	138.04		0.2621	829.90
η	548.80		0.1673*	900.00
η'	957.50		0.1802	900.00
ρ	770.00	0.7794	3.3166	782.38
ω	783.90	3.1242	0.0712	890.23
ϕ	1019.50	−0.6957	1.2686*	890.23
a_1	1270.00	2.4230		968.23
f_1	1420.00	1.4708		968.23
f_1'	1285.00	0.5981*		968.23
a_0	962.00	0.8111		1161.27
ε	760.00	2.8730		1101.62
f_0	993.00	−0.9669		1101.62
a_2	309.10	0.0000		
Pomeron	309.10	2.2031		

B. Coupling constants

In Table VI we show the OBE coupling constants and the Gaussian cutoffs Λ. The used $\alpha =: F/(F+D)$ ratios for the OBE couplings are pseudoscalar mesons $\alpha_{pv} = 0.388$; vector mesons $\alpha_V^e = 1.0, \alpha_V^m = 0.387$; and scalar mesons $\alpha_S = 0.852$, which is computed by using the physical $S^* = f_0(993)$ coupling etc. In Table VII we show the MPE coupling constants. The used $\alpha =: F/(F+D)$ ratios for the MPE couplings are $(\pi\eta)$, etc. $(\pi\omega)$ pairs $\alpha(\{8_s\}) = 1.0, (\pi\pi)_1$, etc; pairs $\alpha_V^e(\{8\}_a) = 1.0, \alpha_V^m(\{8\}_a) = 0.387, (\pi\rho)_1$ etc; pairs $\alpha_A(\{8\}_a) = 0.652$.

Unlike in Refs. [2,3], we did not fix pair couplings by using a theoretical model, based on heavy-meson saturation and chiral symmetry. So, in addition to the 14 parameters used in Refs. [2,3], we now have 6 pair-coupling fit parameters. In Table VII the fitted pair couplings are given. Note that the $(\pi\pi)_0$ pair coupling gets contributions from the $\{1\}$ and the $\{8_s\}$ pairs as well, giving in total $g_{(\pi\pi)} = 0.10$, which has the same sign as in Ref. [3]. The $f_{(\pi\pi)_1}$ pair coupling has the opposite sign compared with Ref. [3]. In a model with a more complex and realistic meson dynamics [4] this coupling is predicted, as is found in the present ESC fit. The $(\pi\rho)_1$ coupling agrees nicely with A_1 saturation; see Ref. [3]. We conclude that the pair couplings are in general not well understood and deserve more study.

TABLE VII. Pair-meson coupling constants employed in the ESC04 MPE potentials. Coupling constants are at $\mathbf{k}^2 = 0$.

J^{PC}	SU(3) irrep	$(\alpha\beta)$	$g/4\pi$	$f/4\pi$
0^{++}	$\{1\}$	$(\pi\pi)_0$	0.0000	
0^{++}	,,	$(\sigma\sigma)$	—	
0^{++}	$\{8\}_s$	$(\pi\eta)$	−0.440	
0^{++}		$(\pi\eta')$	—	
1^{--}	8_a	$(\pi\pi)_1$	0.000	0.119
1^{++}	,,	$(\pi\rho)_1$	0.835	
1^{++}	,,	$(\pi\sigma)$	0.022	
1^{++}	,,	(πP)	0.0	
1^{+-}	$\{8\}_s$	$(\pi\omega)$	−0.170	

TABLE VIII. χ^2 and χ^2 per datum at the ten energy bins for the Nijmegen93 partial-wave-analysis. $N_{\rm data}$ lists the number of data within each energy bin. The bottom line gives the results for the total 0–350 MeV interval. The χ^2 excess for the ESC model is denoted $\Delta\chi^2$ and $\Delta\hat{\chi}^2$, respectively.

$T_{\rm lab}$	No. of data	χ_0^2	$\Delta\chi^2$	$\hat{\chi}_0^2$	$\Delta\hat{\chi}^2$
0.383	144	137.5549	20.7	0.960	0.144
1	68	38.0187	52.4	0.560	0.771
5	103	82.2257	10.0	0.800	0.098
10	209	257.9946	27.5	1.234	0.095
25	352	272.1971	29.2	0.773	0.083
50	572	547.6727	141.1	0.957	0.247
100	399	382.4493	32.4	0.959	0.081
150	676	673.0548	85.5	0.996	0.127
215	756	754.5248	154.6	0.998	0.204
320	954	945.3772	350.5	0.991	0.367
Total	4233	4091.122	903.9	0.948	0.208

The ESC model described here is fully consistent with SU(3) symmetry. For the full SU(3) contents of the pair interaction Hamiltonians, we refer to paper II, Sec. III. Here, one finds, for example, that $g_{(\pi\rho)_1} = g_{A_8VP}$, and besides $(\pi\rho)$ pairs one sees also that $(KK^*(I=1)$ and $KK^*(I=0)$ pairs contribute to the NN potentials. All $F/(F+D)$ ratios are taken to be fixed with heavy-meson saturation in mind, which implies that these ratios are 0.4 or 1.0, depending on the heavy-meson type. The approximation we have made in this paper is to neglect the baryon mass differences; i.e., we set $m_\Lambda = m_\Sigma = m_N$. This because we have not yet worked out the formulas for the inclusion of these mass differences, which is straightforward in principle.

VI. DISCUSSION AND CONCLUSIONS

We mentioned that we do not include negative-energy-state contributions. It is assumed that strong pair suppression is operative at low energies in view of the composite nature of the nucleons. This leaves for us the pseudoscalar mesons with two essential equivalent interactions: The direct and the derivative one. In expanding the $NN\pi$ etc. vertex in $1/M_N$, these two interactions differ in the $1/M_N^2$ terms; see Ref. [2], Eqs. (3.4) and (3.5). This gives the possibility of using instead of the interaction in Eq. (3.1) the linear combination

$$\mathcal{H}_{ps} = \tfrac{1}{2}[(1-a_{PV})g_{NN\pi}\bar{\psi}i\gamma_5\boldsymbol{\tau}\psi\cdot\boldsymbol{\pi} + a_{PV}(f_{NN\pi}/m_\pi)\gamma_\mu\gamma_5\boldsymbol{\tau}\psi\cdot\partial^\mu\boldsymbol{\pi}], \qquad (6.1)$$

where $g_{NN\pi} = (2M_N/m_\pi)f_{NN\pi}$. In ESC04 we have fixed $a_{PV} = 1$, i.e., a purely derivative coupling.

The presented ESC model is successful in describing the NN data, even in this QPC-constrained version. Allowing total freedom in the couplings and cutoff masses, and without fitting the low-energy parameters, we reached the lowest

$\chi^2_{p.d.p.} = 1.10$. However, in that case some couplings look rather artificial. With less freedom, a typical fit with the ESC model has $\chi^2_{p.d.p.} = 1.15$, see e.g., Ref. [5]. This means that by constraining the parameters rather strongly, in the present *NN*-model ESC04 we we reached $\chi^2_{p.d.p.} = 1.155$, i.e., we have only an extra $\Delta\chi^2 \approx 250$, showing the feasibility of the QPC-inspired couplings.

The advantage of this is that we have physically motivated OBE couplings etc. We will see in the next paper of this series, where we study the $S = -1$ *YN* channels, that this feature persists when we fit *NN* and *YN* simultaneously. Then the advantage is that, going to the $S = -2$ *YN* and *YY* channels, it is reasonable to believe that the predictions made for these channels are realistic ones. So far, there did not exist a realistic *NN* model with sizable axial-vector mesons couplings as predicted by Schwinger [19]. Also, the zero in the scalar form factor has moderated the $f_0(760)$ coupling such that it fits with the QPC model.

A momentum-space version of ESC04 is readily available, using the material in Ref. [5]. We only have to add the momentum-space potentials for the axial-vector mesons and the Graz corrections [34], which is rather straightforward.

Finally, the potentials of this paper are available on the Internet [50].

ACKNOWLEDGMENTS

Discussions with Prof. R. A. Bryan, J. J. de Swart, R. G. E. Timmermans, and Drs. G. Erkol and M. Rentmeester are gratefully acknowledged.

APPENDIX: AXIAL-VECTOR-MESON COUPLING TO NUCLEONS

The coupling of the axial mesons ($J^{\rm PC} = 1^{++}$) to the nucleons is given by

$$\begin{aligned}\mathcal{L}_{ANN} &= g_A[\bar\psi\gamma_5\gamma_\mu\boldsymbol{\tau}\psi]\cdot\mathbf{A}^\mu + i\frac{f_A}{\mathcal{M}}[\bar\psi\gamma_5\boldsymbol{\tau}\psi]\cdot\partial_\mu\mathbf{A}^\mu \\ &\approx g_A[\bar\psi\gamma_5\gamma_\mu\boldsymbol{\tau}\psi]\cdot\mathbf{A}^\mu. \end{aligned} \quad \text{(A1)}$$

Here, $\mathcal{M} = 1$ GeV is again a scaling mass. We note that with $f_A = 0$ this coupling is part of the A_1 interaction with pions and nucleons,

$$\mathcal{L}_I = 2g_A\left[\bar\psi\gamma_5\gamma_\mu\tfrac{1}{2}\boldsymbol{\tau}\psi + (\boldsymbol{\pi}\partial_\mu\sigma - \sigma\partial_\mu\boldsymbol{\pi}) + f_\pi\partial_\mu\boldsymbol{\pi}\right]\cdot\mathbf{A}^\mu,$$

which is such that the A_1 couples to an almost conserved axial current (PCAC). Therefore the A_1 coupling used here is compatible with broken $\mathrm{SU}(2)_V \times \mathrm{SU}(2)_A$ symmetry; see, e.g., Refs. [20,51]. For a more complete discussion of the A_1 couplings to baryons, we refer to Ref. [4]. The latter reveals that as far as the axial-nucleon-nucleon coupling is concerned it is indeed of the type indicated above.

In the Proca formalism, for the axial-vector propagator the polarization sum enters:

$$\Pi^{\mu\nu}(k) = \sum_\lambda \epsilon^\mu(k,\lambda)\epsilon^\nu(k,\lambda) = -\eta^{\mu\nu} + k^\mu k^\nu/m^2, \quad \text{(A2)}$$

where m denotes the mass of the axial meson and $\epsilon^\mu(k)$ the polarization vector. Because

$$[\bar\psi\gamma_5\gamma_\mu\psi]k^\mu k^\nu[\bar\psi\gamma_5\gamma_\nu\psi] = [-i\bar\psi\gamma_5\gamma_\mu k^\mu\psi][+i\bar\psi\gamma_5\gamma_\nu k^\nu\psi], \quad \text{(A3)}$$

the second term in the propagator gives potentials that are exactly of the form of those of pseudo vector exchange. We note that these $\Gamma_5(p',\,p) = \gamma_5\gamma\cdot k$ factors come from the ∂^μ derivative of the pseudo vector baryon current. Then,

$$\begin{aligned}&\bar u(p')\Gamma_5(p',\,p)u(p) \\ &\quad\approx i\left[\boldsymbol{\sigma}\cdot(\mathbf{p}-\mathbf{p}') \mp \frac{E(\mathbf{p})-E(\mathbf{p}')}{2M}\boldsymbol{\sigma}\cdot(\mathbf{p}+\mathbf{p}')\right], \end{aligned} \quad \text{(A4)}$$

in contrast to what is used in Ref. [21], where in the $1/M$-term $\omega(\mathbf{k})$ is taken, instead of the baryon energy difference. Notice that the second term in Eq. (A4) is of order $1/M^2$ and moreover vanishes for the on energy shell. Hence we neglect this term. We write

$$\tilde V_A = \tilde V_A^{(1)} + \tilde V_A^{(2)}, \quad \text{(A5)}$$

where $\tilde V_A^{(2)} = \tilde V_{PV}$ with $f_{PV}^2/m_\pi^2 \to g_A^2/m^2$. The transformation to the Lippmann-Schwinger equation implies the potential

$$\tilde{\mathcal{V}}_A \cong \left(1 - \frac{\mathbf{k}^2}{8M'M} - \frac{\mathbf{q}^2}{2M'M}\right)\tilde V_A. \quad \text{(A6)}$$

Below, $M' = M_N$ and $M = M_Y$ are the average nucleon mass or an average hyperon mass, depending on the baryon-baryon system.

A. $\mathcal{V}_A^{(1)}$ potential term

With restriction to terms that are at most of order $1/M^2$, we solve for the potential in Pauli-spinor space for the Lippmann-Schwinger equation for $\tilde{\mathcal{V}}_A^{(1)}$. Note here that, especially for the anti-spin-orbit term, that $(M, \boldsymbol{\sigma}_1)$ and $(M', \boldsymbol{\sigma}_2)$ go with line 1 and line 2, respectively. Defining

$$\mathbf{k} = \mathbf{p}' - \mathbf{p}, \qquad \mathbf{q} = \tfrac{1}{2}(\mathbf{p}' + \mathbf{p}) \quad \text{(A7)}$$

and moreover using the approximation

$$\frac{1}{M^2} + \frac{1}{M'^2} \approx \frac{2}{MM'}, \quad \text{(A8)}$$

we see that the potential $\mathcal{V}_A^{(1)}$ is given in momentum space by

$$\begin{aligned}\tilde{\mathcal{V}}_A^{(1)} = -g_A^2\Bigg\{&\left(1 + \frac{(\mathbf{q}^2+\mathbf{k}^2/4)}{6M'M}\right)\boldsymbol{\sigma}_1\cdot\boldsymbol{\sigma}_2 \\ &+ \frac{2}{MM'}\left[(\boldsymbol{\sigma}_1\cdot\mathbf{q})(\boldsymbol{\sigma}_2\cdot\mathbf{q}) - \frac{1}{3}\mathbf{q}^2\boldsymbol{\sigma}_1\cdot\boldsymbol{\sigma}_2\right] \\ &- \frac{1}{4M'M}\left[(\boldsymbol{\sigma}_1\cdot\mathbf{k})(\boldsymbol{\sigma}_2\cdot\mathbf{k}) - \frac{1}{3}\mathbf{k}^2\boldsymbol{\sigma}_1\cdot\boldsymbol{\sigma}_2\right] \\ &+ \left(\frac{1}{4M^2} - \frac{1}{4M'^2}\right)\cdot\frac{i}{2}(\boldsymbol{\sigma}_1 - \boldsymbol{\sigma}_2)\cdot\mathbf{q}\times\mathbf{k} \\ &+ \frac{i}{4M'M}(\boldsymbol{\sigma}_1 + \boldsymbol{\sigma}_2)\cdot\mathbf{q}\times\mathbf{k}\Bigg\}\cdot\left(\frac{1}{\omega^2}\right), \end{aligned} \quad \text{(A9)}$$

Now, for a complete treatment one has to deal with the nonlocal tensor. Although this can be done, see notes on nonlocal tensor potentials in Ref. [37]; in this work we use an approximate treatment. We neglect the purely nonlocal tensor potential by making in Eq. (A9) the substitution

$$\frac{1}{MM'}\left[(\boldsymbol{\sigma}_1\cdot\mathbf{q})(\boldsymbol{\sigma}_2\cdot\mathbf{q})-\frac{1}{3}\mathbf{q}^2\boldsymbol{\sigma}_1\cdot\boldsymbol{\sigma}_2\right]$$

$$\rightarrow\ -\frac{1}{4MM'}\left((\boldsymbol{\sigma}_1\cdot\mathbf{k})(\boldsymbol{\sigma}_2\cdot\mathbf{k})-\frac{1}{3}\mathbf{k}^2\boldsymbol{\sigma}_1\cdot\boldsymbol{\sigma}_2\right), \quad \text{(A10)}$$

leading to a potential with only a nonlocal spin-spin term. With this approximation, Eq. (A9) becomes

$$\begin{aligned}\tilde{\mathcal{V}}_A^{(1)} = -g_A^2\Bigg\{&\left(1+\frac{(\mathbf{q}^2+\mathbf{k}^2/4)}{6M'M}\right)\boldsymbol{\sigma}_1\cdot\boldsymbol{\sigma}_2\\ &-\frac{3}{4M'M}\left[(\boldsymbol{\sigma}_1\cdot\mathbf{k})(\boldsymbol{\sigma}_2\cdot\mathbf{k})-\frac{1}{3}\mathbf{k}^2\boldsymbol{\sigma}_1\cdot\boldsymbol{\sigma}_2\right]\\ &+\left(\frac{1}{4M^2}-\frac{1}{4M'^2}\right)\cdot\frac{i}{2}(\boldsymbol{\sigma}_1-\boldsymbol{\sigma}_2)\cdot\mathbf{q}\times\mathbf{k}\\ &+\frac{i}{4M'M}(\boldsymbol{\sigma}_1+\boldsymbol{\sigma}_2)\cdot\mathbf{q}\times\mathbf{k}\Bigg\}\cdot\left(\frac{1}{\omega^2}\right). \quad \text{(A11)}\end{aligned}$$

Then, we find in configuration space

$$\begin{aligned}\mathcal{V}_A^{(1)} = -\frac{g_A^2}{4\pi}m\Bigg[&\phi_C^0(m,r)(\boldsymbol{\sigma}_1\cdot\boldsymbol{\sigma}_2)\\ &-\frac{1}{12M'M}\left(\nabla^2\phi_C^0+\phi_C^0\nabla^2\right)(m,r)(\boldsymbol{\sigma}_1\cdot\boldsymbol{\sigma}_2)\\ &+\frac{3m^2}{4M'M}\phi_T^0(m,r)S_{12}+\frac{m^2}{2M'M}\phi_{\rm SO}^0(m,r)\mathbf{L}\cdot\mathbf{S}\\ &+\frac{m^2}{4M'M}\frac{M'^2-M^2}{M'M}\phi_{\rm SO}^{(0)}(m,r)\cdot\frac{1}{2}(\boldsymbol{\sigma}_1-\boldsymbol{\sigma}_2)\cdot\mathbf{L}\Bigg]. \quad \text{(A12)}\end{aligned}$$

B. $\mathcal{V}_A^{(2)}$ potential term

For the PV-type contributions we have [34]

$$\begin{aligned}\tilde{\mathcal{V}}_A^{(2)} = -\frac{g_A^2}{m^2}&\left(1-\frac{\mathbf{k}^2}{8M'M}-\frac{\mathbf{q}^2}{2M'M}\right)\\ &\times(\boldsymbol{\sigma}_1\cdot\mathbf{k})(\boldsymbol{\sigma}_2\cdot\mathbf{k})\left(\frac{1}{\omega^2}\right). \quad \text{(A13)}\end{aligned}$$

The corresponding potentials in configuration space are

$$\begin{aligned}\mathcal{V}_A^{(2)} = \frac{g_A^2}{4\pi}m\Bigg[&\frac{1}{3}(\boldsymbol{\sigma}_1\cdot\boldsymbol{\sigma}_2)\phi_C^1+\frac{1}{12M'M}(\boldsymbol{\sigma}_1\cdot\boldsymbol{\sigma}_2)\\ &\times\left(\nabla^2\phi_C^1+\phi_C^1\nabla^2\right)+S_{12}\phi_T^0\\ &+\frac{1}{4M'M}\left(\nabla^2\phi_T^0S_{12}+\phi_T^0S_{12}\nabla^2\right)\Bigg]. \quad \text{(A14)}\end{aligned}$$

[1] T. A. Rijken, *Proceedings of the XIVth European Conference on Few-Body Problems in Physics*, Amsterdam 1993, edited by B. Bakker and R. von Dantzig, Few-Body Systems, Suppl. **7**, 1 (1994).
[2] T. A. Rijken and V. G. J. Stoks, Phys. Rev. C **54**, 2851 (1996).
[3] T. A. Rijken and V. G. J. Stoks, Phys. Rev. C **54**, 2869 (1996).
[4] V. G. J. Stoks and T. A. Rijken, Nucl. Phys. **A613**, 311 (1997).
[5] T. A. Rijken, H. Polinder, and J. Nagata, Phys. Rev. C **66**, 044008 (2002); **66**, 044009 (2002).
[6] T. A. Rijken, *Proceedings of the 1st Asian-Pacific Conference on Few-Body Problems in Physics*, Tokyo 1999 (to be published).
[7] T. A. Rijken, *Proceedings of the Seventh International Conference on Hypernuclear and Strange Particle Physics* [Nucl. Phys. **A691**, 322c (2001)].
[8] P. M. M. Maessen, T. A. Rijken, and J. J. de Swart, Phys. Rev. C **40**, 2226 (1989).
[9] T. A. Rijken, V. G. J. Stoks, and Y. Yamamoto, Phys. Rev. C **59**, 21 (1999).
[10] T. A. Rijken and Y. Yamamoto, *Extended-soft-core Baryon-Baryon Model, II. Hyperon-Nucleon Scattering*, Phys. Rev. C **73**, 044008 (2006).
[11] T. A. Rijken and Y. Yamamoto, *Extended-soft-core Baryon-Baryon Model, III. Hyperon-Nucleon Scattering $S=-2$*, 2006 (in preparation).
[12] A. Manohar and H. Georgi, Nucl. Phys. **B234**, 189 (1984); H. Georgi, Annu. Rev. Nucl. Part. Sci. **43**, 209 (1993).
[13] J. Polchinsky, Nucl. Phys. **B231**, 269 (1984).
[14] M. M. Nagels, T. A. Rijken, and J. J. de Swart, Phys. Rev. D **17**, 768 (1978).
[15] J. J. de Swart, P. M. M. Maessen, T. A. Rijken, and R. G. E. Timmermans, Nuovo Cimento A **102**, 203 (1989).
[16] L. Micu, Nucl. Phys. **B10**, 521 (1969); R. Carlitz and M. Kislinger, Phys. Rev. D **2**, 336 (1970).
[17] A. Le Yaouanc, L. Oliver, O. Péne, and J.-C. Raynal, Phys. Rev. D **8**, 2223 (1973).
[18] A. Le Yaouanc, L. Oliver, O. Péne, and J.-C. Raynal, Phys. Rev. D **11**, 1272 (1975).
[19] J. Schwinger, Phys. Rev. **167**, 1432 (1968); Phys. Rev. Lett. **18**, 923 (1967).
[20] J. Schwinger, *Particles and Sources* (Gordon & Breach, New York, 1969).
[21] T. A. Rijken, Ann. Phys. (NY) **208**, 253 (1991).
[22] A. Klein, Phys. Rev. **90**, 1101 (1952); W. Macke, Z. Naturforsch. **89**, 599 (1953); **89**, 615 (1953).
[23] R. P. Feynman, Phys. Rev. **76**, 769 (1949).
[24] J. Schwinger, Proc. Natl. Acad. Sci. USA **37**, 452 (1951).
[25] E. Salpeter and H. A. Bethe, Phys. Rev. **84**, 1232 (1951).
[26] P. A. Carruthers, *Spin and Isospin in Particle Physics* (Gordon & Breach, New York, 1971).
[27] J. D. Bjorken and S. D. Drell, *Relativistic Quantum Fields* (McGraw-Hill, New York, 1965). We follow the conventions of this reference, except for $(-)$ sign in the definition Eq. (2.5) of the M matrix. The later is customary in works that employ potentials.

[28] A. Klein and T.-S. H. Lee, Phys. Rev. D **12**, 4308 (1974).
[29] R. H. Thompson, Phys. Rev. D **1**, 110 (1970).
[30] E. Salpeter, Phys. Rev. **87**, 328 (1952).
[31] M. M. Nagels, T. A. Rijken, and J. J. de Swart, Phys. Rev. D **15**, 2547 (1977).
[32] J. J. de Swart, M. M. Nagels, T. A. Rijken, and P. A. Verhoeven, Springer Tracts Mod. Phys. **60**, 138 (1971).
[33] At this point it is suitable to change the notation of the initial and final momenta. We use from now on the notation $\mathbf{p}_i \equiv \mathbf{p}$, $\mathbf{p}_f \equiv \mathbf{p}'$ for both on-shell and off-shell momenta.
[34] M. M. Nagels, T. A. Rijken, and J. J. de Swart, *Few Body Systems and Nuclear Forces I, Proceedings Graz 1978*, edited by H. Zingl, M. Haftel, and H. Zankel, Vol. 82 of Lecture Notes in Physics (Springer, Berlin Heidelberg New York, 1978), p. 2.
[35] K. A. Bruckner and K. M. Watson, Phys. Rev. **92**, 1023 (1953).
[36] M. Taketani, S. Machida, and S. Ohnuma, Prog. Theor. Phys. **7**, 52 (1952).
[37] T. A. Rijken, "General non-local potentials," http://nn-online.org/04.02, 2004.
[38] R. van Royen and V. F. Weisskopf, Nuovo Cimento A **50**, 617 (1967).
[39] E. Leader and E. Predazzi, *An Introduction to Gauge Theories and Modern Particle Physics*, Cambridge Monographs on Particle Physics, Nuclear Physics and Cosmology, edited by T. Ericson and P. V. Landshoff (Cambridge University Press, Cambridge, 1996), Vol I, Chap. 12.
[40] M. Chaichian and R. Kögerler, Ann. Phys. **124**, 61 (1980).
[41] Particle Data Group (PDG), "*Review of Particle Physics*," Phys. Rev. D **66** 010001-1 (2002). More sophisticated formulas for $\alpha_s(\mu)$ can be found in more recent publications of the PDG. In view of the rather qualitative character of the discussion here, the formula used is adequate.
[42] R. A. Bryan and A. Gersten, Phys. Rev. D **6**, 341 (1972).
[43] V. G. J. Stoks, R. A. M. Klomp, M. C. M. Rentmeester, and J. J. de Swart, Phys. Rev. C **48**, 792 (1993).
[44] D. V. Bugg and R. A. Bryan, Nucl. Phys. **A540**, 449 (1992).
[45] R. A. M. Klomp (private communication).
[46] V. G. J. Stoks, R. A. M. Klomp, C. P. F. Terheggen, and J. J. de Swart, Phys. Rev. C **49**, 2950 (1994).
[47] D. E. Gonzalez Trotter, F. Salinas, Q. Chen, A. S. Crowell, W. Glöckle, C. R. Howell, C. D. Roper, D. Schmidt, I. Šlaus, H. Tang, W. Tornow, R. L. Walter, H. Witala, and Z. Zhou, Phys. Rev. Lett. **83**, 3788 (1999).
[48] V. Huhn, L. Wätzold, Ch. Weber, A. Siepe, W. von Witsch, H. Witala, and W. Glöckle, Phys. Rev. Lett. **85**, 1190 (2000).
[49] G. A. Miller, B. M. K. Nefkens, and I. Slaus, Phys. Rep. **194**, 1 (1990).
[50] ESC04 *NN* potentials, see: http://nn-online.org
[51] V. De Alfaro, S. Fubini, G. Furlan, and C. Rosetti, *Currents in Hadron Physics* (North-Holland, Amsterdam, 1973).